This is to certify that the

thesis entitled

NON-SHEAR COMPLIANCES AND ELASTIC CONSTANTS FOR NINE HARDWOOD TREES

presented by

YING YU

has been accepted towards fulfillment
of the requirements for

M.S. degree in FORESTRY

Alan Sliker
Major professor

Date Oct 18, 1990

DATE DUE	DATE DUE	DATE DUE

NON-SHEAR COMPLIANCES AND ELASTIC CONSTANTS MEASURED FOR NINE HARDWOOD TREES

By

Ying Yu

A THESIS

Submitted to
Michigan State University
in partial fulfillment of the requirements
for the degree of

MASTER OF SCIENCE

Department of Forestry

1990

ABSTRACT

NON-SHEAR COMPLIANCES AND ELASTIC CONSTANTS FOR NINE HARDWOOD TREES

By

Ying Yu

Non-shear compliances (S_{LL}, S_{RL}, S_{TL}, S_{RR}, S_{LR}, S_{TR}, S_{TT}, S_{LT}, S_{RT}), Young's moduli (E_L, E_R, and E_T), and Poisson's ratios (ν_{LR}, ν_{LT}, ν_{RL}, ν_{RT}, ν_{TL}, ν_{TR}) were measured at a single moisture content condition using matched samples from nine trees representing six hardwood species. Linear relationships were found between pairs of compliances from the loading of specimens in a given direction (L, R, or T). Most equations were in agreement with previous equations determined by Sliker. Except for ν_{RL} there was also good agreement in values for Poisson's ratios. ν_{LR} and ν_{LT} appeared to have the same value for all species. There also appeared to be good agreement between data for S_{LL}, S_{RR}, and S_{TT} and empirical equations relating these compliances.

ACKNOWLEDGMENTS

I would like to express sincere appreciation to Dr. Alan W. Sliker, my major advisor, for his great patience and enthusiasm in the guidance and assistance throughout this study. Also, my sincere gratitude was extended to Dr. Sliker for providing me the funds which made this study possible.

Thanks go to my graduate committee members, Dr. Otto M. Suchsland and Dr. Nicholas J. Altiero for giving me helpful suggestions and guidances.

I also thank Mr. Timothy G. Weigel for his assistance in the experiment.

Finally, I express my hearty thanks to my husband, Zhijun Liu, and my daughter, Mei Liu, for their encouragement and support all the way through my degree. Hearty thanks go to my parents and grandmother for their understanding and moral support of my study abroad.

TABLE OF CONTENTS

LIST OF TABLES

LIST OF TABLES CONTINUED

LIST OF TABLES CONTINUED

LIST OF FIGURES

LIST OF FIGURES CONTINUED

Page

LIST OF FIGURES CONTINUED

Page

NOTATION

i = subscript L, R, or T.

j = subscript L, R, or T.

L, R, T = longitudinal, radial and tangential axes.

E_i = Young's modulus in the i direction.

G_{ij} = shear modulus of elasticity in the ij plane, $i \neq j$.

S_{ij} = compliance with strain in the i direction per unit stress in the j direction for loading in the j direction.

ν_{ji} = Poisson's ratio with strain in the i direction to that in the j direction for loading in the j direction; $i \neq j$.

σ_i = stress in the i direction.

ε_i = strain in the i direction.

INTRODUCTION

The work described here is part of a larger program to collect data on the non-shear compliances of wood from the testing of wood in compression in the longitudinal(L), radial(R), and tangential(T) directions. An ultimate objective of this research is to find all the non-shear compliances as functions of the reciprocal of Young's modulus in the L direction ($1/E_L$). Previously (Sliker, 1985, 1988, and 1989), data was collected for comparing compliances, which resulted in the finding of linear relationships between pairs of compliances. In that testing, specimens for loading in the L, R, and T directions were not matched with respect to trees or species, which made a statistical analysis of the relationships between all the compliances and $1/E_L$ more difficult. It is hoped that the use of matched samples as in this report will help clarify the desired relationships. In addition to the samples from nine trees tested for this thesis, another set of samples from nine additional trees is also being tested. The results of the two sets of data will be combined for a final comprehensive analysis.

Wood is cellular biological material, which can be divided into two categories, hardwood and softwood.

Hardwood is the product of broad-leaved species (dicotyledons of the Angiosperms), and softwood is the product of coniferous trees (conifers of Gymnosperms) (Core et al., 1979). This study emphasized the hardwoods. Hardwoods are also called porous woods because of their possessing vessel elements, which can be viewed in the transverse section as pores. Based on the change or lack of change of pore size across the growth ring, hardwoods can be separated into two groups, ring-porous woods and diffuse-porous woods (Core et al., 1979). Ring-porous species displays distinct layers of large pore portion which is composed of large, thin-wall cells. Because this portion is generally formed at the early part of the growth season, it is called early-wood or spring-wood. In the late season, actually starting in summer, layers of cells featured with small, thick-wall pores are produced by the cambium of a living tree. This portion is called late-wood or summer-wood. Early-wood and late-wood form the annual growth ring (growth increment). Oak and ash are in this category. Diffuse-porous species differ in the fact that vessels are generally uniformly distributed within an annual growth ring so that there is no distinct boundaries between early-wood and late-wood. Examples for this category are maple and yellow-poplar. Some woods, such as cottonwood and walnut, are intermediate between ring-porous and diffuse-porous woods, and thus classed as semi-ring-porous or semi-diffuse-porous woods (Panshin and De Zeeuw, 1970). One of the most distinct visual characteristics among woods is whether they are ring-porous, diffuse-porous, or semi-ring-porous species.

Woods from different species show large variations in physical properties due to the variations in cell dimensions and cell wall thicknesses. Woods from different trees of the same species are also likely to show variations in physical properties due to different growth conditions and genetic variations. Even within a tree, variations exist. In the central region of a tree near the pith, wood is called juvenile wood (Panshin and De Zeeuw, 1970). The rest of the wood formed away from pith is called mature wood. Juvenile wood and mature wood are quite different in physical properties because of the differences in cell structure and growth ring width. Usually, juvenile wood has wider growth ring than mature wood.

Wood is anisotropic so that physical properties are different when tested along its three major directions L, R, and T. In order to get the non-shear compliances of wood in compression in the L, R, and T directions, truly orthotropic surfaces on a specimen should be made. This is quite difficult. Wood boards usually have to be resawn to obtain truly radial and tangential surfaces, since most boards are not truly aligned to these surface. For test specimens, wood grain needs to be as straight as possible on the radial and tangential surfaces. The annual growth rings on the cross-sectional surfaces should have as little curvature as possible. Even when specimens are perfectly aligned with respect to orthotropic axes, there can be large variation in properties in any direction due to change in cell types, change in cell wall thickness of a given cell type, variability in growth ring width and the presence of abnormal wood such as tension wood in hardwoods.

There are some problems in using commercially produced gages on wood to measure the strains since these gages are principally designed for use on metals. First, the stiffness of a strain gage can produce a significant reinforcing effect when the gage is installed on a material with a low elastic modulus (Perry, 1985). Wood in the R and T directions belongs to the low elastic modulus material. Most commercial strain gages are stiffer than wood so that movement of wood is restrained under the gages. Secondly, "when most commercial types of bonded electrical resistance strain gages are used on dielectric materials, undesirable drifts of the gages occur as they are energized in the measuring circuit"(Sliker, 1959). These are mainly due to the poor heat dissipation properties of wood and the accumulation of heat in the vicinity of the gages. Drift of gages is generated by the thermal expansion of either the gage itself or the wood or both the gage and the wood, so it is called thermal drift. Shrinkage of the wood underneath the gage may also occur due to the heating of the wood.

In order to overcome these problems caused by commercial produced gages, it is desirable to make our own bonded wire electrical resistance strain gages for use in wood strain tests. These gages have no backing material such as paper or plastic, which greatly add to the stiffness of commercial gages. The wire used to make gages is very thin and does not add much restraining effect to the wood. And the gages are made with only one or two strands or have a comparatively wide spacing between adjacent strands to reduce heat concentration (Sliker, 1959).

There are twelve elastic constants and related compliances for wood, which correspond with three major orthotropic surfaces. The elastic constants are Young's moduli in the L, R, and T directions--E_L, E_R, and E_T; six Poisson's ratios--ν_{LR}, ν_{LT}, ν_{RT}, ν_{RL}, ν_{TR}, ν_{TL}; and three shear moduli G_{LR}, G_{LT}, G_{RT}. The compliances are combinations of the elastic constants as indicated in the next paragraph for the non-shear compliances. The only elastic constant that is readily available for use in structural design for most species is E_L. It is difficult to obtain appropriate values for the other elastic constants (Sliker, 1988). Because of developments in scientific test equipment and computer technology in the 80's, the difficulty could be solved.

In order to show three dimensional relationship of strain to stress for an orthotropic material, a matrix equation can be written in terms of compliances or the engineering elastic parameters (Bodig and Jayne, 1982):

$$\begin{bmatrix} \varepsilon_L \\ \varepsilon_R \\ \varepsilon_T \end{bmatrix} = \begin{bmatrix} S_{LL} & S_{LR} & S_{LT} \\ S_{RL} & S_{RR} & S_{RT} \\ S_{TL} & S_{TR} & S_{TT} \end{bmatrix} \begin{bmatrix} \sigma_L \\ \sigma_R \\ \sigma_T \end{bmatrix} = \begin{bmatrix} 1/E_L & -\nu_{RL}/E_R & -\nu_{TL}/E_T \\ -\nu_{LR}/E_L & 1/E_R & -\nu_{TR}/E_T \\ -\nu_{LT}/E_L & -\nu_{RT}/E_R & 1/E_T \end{bmatrix} \begin{bmatrix} \sigma_L \\ \sigma_R \\ \sigma_T \end{bmatrix}$$

This also can be written into the following form:

$$\begin{bmatrix} \varepsilon_L \\ \varepsilon_R \\ \varepsilon_T \end{bmatrix} = \begin{bmatrix} \varepsilon_L/\sigma_L & -\varepsilon_L/\sigma_R & -\varepsilon_L/\sigma_T \\ -\varepsilon_R/\sigma_L & \varepsilon_R/\sigma_R & -\varepsilon_R/\sigma_T \\ -\varepsilon_T/\sigma_L & -\varepsilon_T/\sigma_R & \varepsilon_T/\sigma_T \end{bmatrix} \begin{bmatrix} \sigma_L \\ \sigma_R \\ \sigma_T \end{bmatrix}$$

In a previous study, Bodig and Goodman (1973) reported the information about determining the elastic parameters for 18 softwood species from his own data and the other data from Hearmon by plate-bending and plate-twisting method. As an exponential expression, the relationship between the combination of density and elastic parameters showed significant regression within these parameters, except Poisson's ratios, which were constant. Also, E_L might be used to predict the other five elastic parameters, excluding Poisson's ratios.

In 1987, Guitard and Amri found significant multiregressions within the following parameters: specific gravity and elastic properties for 80 different wood species. The complete elastic compliance matrix for a certain wood could be predicted. However, the data used was a mixture from many sources done by different methods.

Sliker had tested a broad range of species which included hardwoods and softwoods as loaded in the three major directions L, R, and T to obtain non-shear elastic constants and related compliances in 1985, 1988, and 1989.

His researches have found the following results at a controlled room condition with 68°F temperature and 65% relative humidity(RH):

$$\begin{array}{lll}
1.\ S_{RL} = 0.022 \times 10^{-6} - 0.405\ S_{LL} & R^2 = 0.900 & \\
2.\ S_{TL} = 0.021 \times 10^{-6} - 0.500\ S_{LL} & R^2 = 0.925 & \\
3.\ S_{TR} = 1.260 \times 10^{-6} - 0.887\ S_{RR} & R^2 = 0.911 & (1) \\
4.\ S_{LR} = 0.029 \times 10^{-6} - 0.0483\ S_{RR} & R^2 = 0.593 & \\
5.\ S_{RT} = -0.659 \times 10^{-6} - 0.255\ S_{TT} & R^2 = 0.980 & \\
6.\ S_{LT} = -0.022 \times 10^{-6} - 0.0274\ S_{TT} & R^2 = 0.980 &
\end{array}$$

Equilibrium moisture content of specimens that were tested by him was between 9 and 12%. In 1990, test specimens were loaded in the L, R, and T directions at three different moisture conditions--40% RH and 68°F, 65% RH and 68°F, 83% RH and 80°F to examine the effect of moisture contents on relationships of non-shear compliances. The EMC of specimens were 5-9%, 9-12%, and 15-20% with respect to the three moisture conditions. Results showed that moisture contents had very little effect on the relationships between pairs of compliances (Sliker et al., in press).

The current study focuses on finding the non-shear compliances for wood from nine different trees, which all belong to hardwood species, using matched samples for loading in the L, R, and T directions. Emphasis will be placed on analyzing the variability of individual measurements and on how well the data fits the Equations 1, which have already been published. Because of the use of matched samples, this new data set also provides an opportunity to compare relationships between $1/E_R$ and $1/E_L$ and between $1/E_T$ and $1/E_L$, and to make a rigorous statistical analysis of subsample differences (Sliker et al., in press). Ultimately the data from this thesis will be combined with that from another thesis to provide another estimate of the relationships between pairs of non-shear compliances and between all the non-shear compliances and $1/E_L$.

MATERIALS AND METHODS

The test material was selected from nine trees and six species, which were cottonwood(*Populus deltoides* S.), hard maple(*Acer* species), red oak(*Quercus* species), soft maple(*Acer* species), white oak(*Quercus* species), and yellow-poplar(*Liriodendron tulipifera* L.). There were two red oaks, two soft maples, and two yellow-poplars among them (see Table 1). The diameters of the trees were over 30 inches. Only mature wood was used for test specimens by selecting only wood which was at least 15 growth rings (preferably 20 or more) from the pith. The trees were all sawn into three and half inches thick planks and then dried in a kiln for about 30 days with a slow schedule to reduce drying defects. For each tree, three types of specimens and a moisture content (MC) sample for each type of test specimen were made according to three different loading directions--longitudinal(L), radial(R), and tangential(T). In order to make truly orthotropic surfaces for each specimen, the boards were resawn to follow grain and to have truly radial and tangential surfaces. For woods where the grain direction was hard to see, a red dye in kerosene was placed on the woods to see its major direction of flow. Each type of specimen has a matched sample in order to make possible a rigorous statistical analysis of subsample differences (Sliker et al., in press). After kiln-drying, a wood block from each board where the specimens were made was cut, weighed, measured in its dimensions to get its kiln-dry weight and kiln-dry volume, and then dried in an oven at 103°C to obtain its oven-dry weight and oven-dry volume. Based on these values the moisture content and the specific gravity of each test board was obtained at the time of specimen preparation (see Table 1). All of the test specimens and MC samples were weighed after they were made, and the MC samples were weighed again during the test to keep track of moisture contents of specimens (Tables 2-6). Final moisture content conditioning and testing was conducted in a room where temperature and relative humidity were maintained at 68°F and 65%. Equilibrium moisture content for selected types of wood at such an environment was between 7 and 13 percent.

The positions where strain gages were to be installed were drawn on specimens before the gages were placed, and then a thin layer of Duco cement was put on these areas. After the adhesive dried, the specimens were lightly sanded by sandpaper with grit No. 180 to make the areas smooth. Following this step, strain gages were mounted on the specimens in specified patterns for each type of loading.

The specimens loaded in the longitudinal direction were approximately 7 inches (18.78 cm) long and 1.25 by 1.25 inches (or 3.20 by 3.20 cm) in cross-sectional dimensions

(Figure 1). "Great care was taken in trying to have the grain of the wood parallel to the length of the specimen and to have the side surfaces be radial and tangential" (Sliker, 1985). The free-filament strain gages, which were designed by Sliker from 4-inch lengths of 1-mil diameter constantan wire having a resistance of 290 ohms per foot soldered to 12-mil diameter constantan lead wire, were used (Sliker, 1985). "Resultant gage resistance was approximately 97 ohms" (Sliker, 1985). Electrical resistance strain gages bonded on a specimen are shown in Figure 1. The gage along the grain direction of specimens was kept at 2 inches long by making one 360 degree bend in the 1-mil wire around a steel straight pin, and the gage perpendicular to the grain direction was kept 1-inch long by making three 360 degree bends in the 1-mil wire around three steel straight pins (Sliker, 1989) when they were bonded to the specimen with a nitrocellulose adhesive (Duco Cement). The gage construction is demonstrated in Figure 2. "Parallel gages on opposite faces of each specimen were connected in series to make one arm of a Wheatstone bridge" (Sliker, 1985).

The method of making individual specimens that were loaded in either the R or T direction was to take a board and cut from it five pieces measuring 1.5 inches by 1.25 inches by 12 inches with the 12-inch dimension being in the L direction and the 1.25-inch dimension being in either the R or T direction according to the specimen type to be made (Sliker, 1988). Then, these five pieces were laminated with polyvinyl acetate adhesive into blanks measuring 1.5 inches by 6.25 inches by 12 inches (Sliker, 1988). The final size of a specimen was about 6 inches long and 1.25 by 1.25 inches in cross-sectional dimension by machining the blanks to a thickness of 1.25 inches and by cutting 6.25-inch dimension at 1.25-inch intervals in the L direction (Figures 3 and 4) (Sliker, 1988). The free-filament strain gages mentioned before were also used here. Gages were mounted only on the central section of each five-layer laminated specimen with thinned Duco Cement adhesive.

There are two types of gage installations for specimens loaded in the R or T direction. One is shown in Figure 3 for loading in the R direction and the other is shown in Figure 4 for loading in the T direction. The mounting method in Figure 3A and Figure 4A was similar to that for the gages perpendicular to the grain direction of specimens loaded in the L direction (refer to Figure 2B for gage construction). Four gages were mounted per specimen with gages on opposite faces being connected in series to eliminate the recording of bending strains (Sliker, 1988). In Figure 3B and Figure 4B, each specimen has two 4-inch free-filament strain gages installed along either the R or T direction on the opposite sides. The way of the gage installation was similar to that for the gages perpendicular to the grain direction of specimen loaded in the L direction. "Although there might be a slight sensitivity to strain in the L direction in this design, the strain pickup in the L direction would be small compared to those in the R and T directions" (Sliker, 1989). There is a special concern when strain gages are mounted along the L direction while loading in the R or T directions. This is that they may pick up some of the large strains in the R and T directions with a gage oriented to measure the small strain in the L direction (Sliker, 1989). Many commercially produced strain gages with loops perpendicular to the main strain axis have this problem in particular. Therefore, if strain gages were made in which all the strain sensitive wire was oriented in the L direction (Sliker, 1989), that could overcome the problem. This was accomplished by making strain gages with 12-mil diameter constantan leads soldered to 1-inch lengths of 1-mil diameter constantan strain gage wire having a resistance of 290 ohms per foot, then placing four of these gages parallel to each other along the L direction on one side of a specimen's middle section with quarter inch intervals (Sliker, 1989). These four gages were connected in series and then were connected in series with a similar arrangement of 1-inch gages on the opposite side of the specimen (Sliker, 1989). Figure 5 shows the scheme for gage construction. Also, there was another problem, which was amplification of the low signal emanating from the gages in the L direction when the specimens were loaded in the R or T direction (Sliker, 1989). Measurements Group's Model 3800 Wide Range Strain Indicator could solve this problem because it could indicate strain to 10^{-7} inches per inch. Shielded cable was used between the strain gage and the measuring instrument in order to keep the noise to signal ratio low (Sliker, 1989).

Test specimens to be loaded in the L direction were placed in a compression cage (Figure 6) for load application. A tensile force on the compression cage applied a compressive force on the test specimens. A key feature of the compression cage, which was made of steel and aluminum, was the placement of a three-eighth-inch spherical bearing between the top and bottom sections of the compression cage and the blocks that bore on the ends of the test specimen (Bodig and Goodman, 1969). "This allowed rotation of the bearing blocks so that equal pressure would be applied over the ends of the specimens" (Sliker, 1988). "Loosely fitting guides near the ends of the specimen keep it centered on the bearing blocks" (Sliker, 1989). An Instron testing machine 4206 was used for loading specimens with the crosshead speed setting at 0.005 in/min (Figure 7). Three direction strains and load in the L direction were recorded at increments of 50 microstrain in the L direction until it was up to 600 microstrain. The strains were read from the Measurements Group's Model 3800 Wide Range Strain Indicators. The range of maximum loads placed on the specimens is from 1099 pounds on COT1 to 1975 pounds on HM2.

For compression loading in the R and T directions, specimens shown in Figure 3 and 4 were placed into the compression cage described previously. "The upper end of the cage was connected to a structural frame by a universal joint, while a load hanger was suspended from the lower end of the cage through another universal joint" (Sliker, 1989). The scheme is shown in Figure 8. Loads were applied by putting ten 10-pound weights on the suspended hanger in quick succession. Less than two minutes elapsed for a given total loading of 100 pounds. Strain parallel and perpendicular to the loading direction were quickly read from Measurements Group's Model 3800 Wide Range Strain Indicators at zero load and after each 10-pound weight being added (Figure 8). When measuring the small strains in the L direction, the gage factor was changed from 2.050 to 0.2050 for increased sensitivity in strain readings.

RESULTS

Linear regression analysis was applied to the strain versus load data for each specimen in order to obtain a best fit value for the slope used to determine the compliance for the specimen. The coefficients of determination for these equations ranged from 0.986 to nearly perfect. Plots of strain in the L, R, and T directions versus load are given for one test sample in Figure 9. Compliances expressed as S_{LL}, S_{RL}, S_{TL}, S_{RR}, S_{TR}, S_{LR}, S_{TT}, S_{RT}, and S_{LT} were derived from the slopes of the curves of each individual specimen by multiplying the slopes by cross-sectional areas of the specimens, which converts load to stress.

Compliances, Young's moduli, and Poisson's ratios for all test specimens are presented in Tables 2 through 6. Young's moduli E_L, E_R, and E_T are the slopes of strain versus stress where the strain and the stress are measured in the same direction. Poisson's ratios are the slopes of curves of strain perpendicular to the load axis divided by strain parallel to the load axis. The signs for the compliances are reversed from those in previous publications by Sliker in 1985, 1988, and 1989 in order to conform with more traditional practice (Sliker et al., in press); i.e. S_{LL}, S_{RR}, S_{TT}, E_L, E_R, and E_T are shown as positive numbers despite being derived from negative strains. Similarly, S_{RL}, S_{TL}, S_{LR}, S_{TR}, S_{LT}, and S_{RT} are shown as negative numbers despite being determined from positive strains.

Linear relationships can be found between pairs of compliances taken for a given direction (L, R, or T) of loading. Regression equations relating pairs of compliances from the data in Tables 2 through 6 are as follows:

1. $S_{RL} = -0.016 \times 10^{-6} - 0.353\ S_{LL}$ $\quad R^2 = 0.613$
2. $S_{TL} = -0.062 \times 10^{-6} - 0.360\ S_{LL}$ $\quad R^2 = 0.566$
3. $S_{TR} = 1.224 \times 10^{-6} - 0.967\ S_{RR}$ $\quad R^2 = 0.858$
4. $S_{LR} = -0.210 \times 10^{-6} - 0.0143\ S_{RR}$ $\quad R^2 = 0.332$ (2)
5. $S_{RT} = -0.309 \times 10^{-6} - 0.288\ S_{TT}$ $\quad R^2 = 0.936$
6. $S_{LT} = -0.266 \times 10^{-6} - 0.00605\ S_{TT}$ $\quad R^2 = 0.100$

Plots of the data and the associated compliances are given in Figures 10 through 15. The slopes and intercepts of Equation 2 are slightly different from these reported on by Sliker in 1985, 1988, and 1989 (Equation 1) and, also, the R^2 are smaller. Two possible reasons for this are the smaller number of samples involved for any one equation and the concentration of the samples in the higher specific gravity species in the current testing. The additional testing being done for another thesis contains more lower specific gravity species. One of the poorest correlations is between S_{LT} and S_{TT}. If the cottonwood is removed from this set of data, the equation ($S_{LT} = 0.107 \times 10^{-6} - 0.047\ S_{TT}$, $R^2 = 0.455$) becomes more like that on Equation 1.

In order to examine how my data points are distributed around a regression line of each of the Equations 1 established by Sliker in 1985, 1988, and 1989, six graphs are generated that contain my data points along with regression lines for Equation 1 (Figures 16-21). In the plots, the data points from nine trees of this study represent the relationship between the strain perpendicular to the loading direction per unit stress parallel to the load direction and the strain per unit stress parallel to the load direction. Each data point represents the average of two replications. The solid straight lines from the Equations 1 found by Sliker also express the relationship between the same two quantities. The plots show that there is a general agreement between the current experimental data and Sliker's data. Statistical analysis as shown in Table 7 indicates that all of the slopes except for one in Equation 2 are not significantly different from the slopes in Equation 1 at the 95% probability level. In other words, common slopes from the two independent experiments can be found. The one exception is the relationship between S_{LT} and S_{TT}. In addition, the current data for S_{LR} versus S_{RR} does not match well with the regression line from Equation 1. Y-axis intercept rather than slope may account for this. S_{LR} and S_{LT} are the two most difficult compliances to measure.

For an orthotropic material, $S_{RL} = S_{LR}$, $S_{TL} = S_{LT}$, and $S_{TR} = S_{RT}$. In this data, there is very good linear correspondence between S_{TR} and S_{RT}. To a lesser extent there is linear correspondence between S_{RL} and S_{LR} and between S_{TL} and S_{LT}. These latter discrepancies may be because of the greater difficulty in measuring S_{LT} and S_{LR} than in measuring the other compliances or it may be related to different viscoelastic responses in loading parallel and perpendicular to the grain. The accumulation of more data should help to better show that there are solid relationships between all these pairs of compliances.

If assuming $S_{RL} = S_{LR}$, $S_{TL} = S_{LT}$, and $S_{TR} = S_{RT}$, three other equations can be obtained from the Equations 1 found by Sliker:

1. $S_{RR} = 0.145 \times 10^{-6} + 8.39\ S_{LL}$
2. $S_{TT} = -1.57 \times 10^{-6} + 18.25\ S_{LL}$ (3)
3. $S_{RR} = 2.19 \times 10^{-6} + 0.291\ S_{TT}$

By using each of these three equations as a solid straight line and the averaged values of S_{LL}, S_{RR} and S_{TT} from nine trees of this report, three plots are obtained and shown in Figures 22-24. The data points from this study in each plot generally fit the straight line except that the cottonwood data point in Figure 23 is far off the straight line found by Sliker. This suggests that either the value for S_{LT} or S_{TL} for cottonwood is not a representative number.

The statistics of regression analysis is given in Table 8. All the slopes except the ones in the equation relating S_{LR} to S_{RR} and the equation relating S_{LT} to S_{TT} are statistically significant at a minimum of 95% probability level. This indicates that there exist linear relationships between the various pairs of compliances listed in Tables 2, 3, and 5 among nine trees tested in this experiment. This may also suggest that linear relationships between compliances exist in a broader range of hardwood species.

Due to the statistical significance of intercepts in equations 4 and 6 in Table 8, these values can be used in establishing the predictive equations for Poisson's ratios, since they can be determined by quotients of compliances:

$\nu_{RL} = (\varepsilon_L/\sigma_R)/(\varepsilon_R/\sigma_R)$ and $\nu_{TL} = (\varepsilon_L/\sigma_T)/(\varepsilon_T/\sigma_T)$

If each term in equation 4 in Table 8 is divided by S_{RR}, it will become: $S_{LR}/S_{RR} = -\ 0.0143 - 0.210 \times 10^{-6}\ 1/S_{RR}$. The term in the right of the above equation equals the Poisson's ratio ν_{RL}. It is obvious that it can be predicted from S_{RR}.

Similarly, if each term in equation 6 in table 8 is divided by S_{TT}, it will become: $S_{LT}/S_{TT} = -0.00605 - 0.266 \times 10^{-6}\ 1/S_{TT}$. Poisson's ratio ν_{TL} then can be predicted from this equation through the use of S_{TT} obtained experimentally.

The rest of the equations in Table 8 showed that intercepts were not significantly different from zero. Therefore, the best way to estimate these Poisson's ratios could be the averages of the test values (Sliker, 1989). The averaged values and their standard deviations for all Poisson's ratios of all the tested trees are shown in Table 9. In order to compare the Poisson's ratios obtained from this study with those reported by Sliker in 1985, 1988, and

1989, a statistical method (t test) was conducted (Table 9). The Poisson's ratios ν_{LR}, ν_{LT}, ν_{RT}, ν_{TR}, and ν_{TL} derived from current study are not significantly different from those found by Sliker with 95% probability level, and the Poisson's ratio ν_{RL} derived from this report is significantly larger than that found by Sliker with 95% probability (Table 9).

Coefficients of variability (CV) of S_{RR} among individual specimen are listed in Table 10. There are four specimens from each tree for the measurements of compliance S_{RR}, of which two are matched samples with the same gage installation (see Figure 3A) and the other two are also matched samples but with another type of gage installation (see Figure 3B). The coefficients of variation among the nine trees tested range from 0.14% in SM2 to 4.18% in WO1 for specimens shown in Figure 3A and 0 in RO2 to 2.98% in SM1 for specimens shown in Figure 3B.

Coefficients of variability of S_{TT} among individual specimen loaded in the T direction are listed in Table 11. There are four specimens from each tree for measuring S_{TT}, of which two are matched samples with the same gage installation (see Figure 4A) and the other two are matched samples, too, but with another type of gage mounting (see Figure 4B). The variabilities among the nine trees tested range from 1.34% in RO1 to 5.42% in SM1 for specimens shown in Figure 4A and 1.00% in RO1 to 4.90% in YP1 for specimens shown in Figure 4B.

Coefficients of variability (CV) of S_{LL}, S_{RL}, S_{TL}, S_{TR}, S_{LR}, S_{RT}, and S_{LT} among individual specimen are listed in Tables 12 through 18. There are two matched samples from each tree for measuring these compliances. The coefficients of variation of S_{LL}, S_{RL}, S_{TL}, S_{TR}, S_{LR}, S_{RT}, and S_{LT} among the nine trees tested range from 0.60 to 13.61%, 0.33 to 22.22%, 1.43 to 25.93%, 0 to 3.33%, 1.10 to 5.66%, 0 to 3.72%, and 0.49 to 6.88%, respectively.

The experimental data collected was analyzed with the procedure of analysis of variance (ANOVA) to determine the differences existing among the nine tested trees in compliances and elastic constants. Results demonstrated that trees, loaded in compression in the L direction, exhibited significantly different responses in compliances, i.e. S_{LL}, S_{RL}, S_{TL}, and Young's moduli, but did not differ in Poisson's ratios (Table 19). When loaded in compression in the R direction, trees tested showed significant differences in all the parameters investigated, regardless of the orientation of the gage settings (Table 20). Similarly, there were significant differences in the nine trees tested when loaded in compression in the T direction in all the compliances and elastic constants studied, no matter which method was used in the gage installation (Table 21).

Trees that showed significant differences in compliances and elastic constants from the ANOVA tables were further tested for their means with Duncan's t-test. Mean values of compliances and E_L for trees that were loaded in compression in the L direction were presented in Table 22. There is clear exhibition of groups in S_{LL}. COT1, RO2, SM1 and SM2 fell in one group and ranked the highest in the nine trees. SM1 and SM2 are not significantly higher than YP1 and RO1 which, however, were different from COT1 and RO2. YP2, WO1, and HM2 belonged to the same group and showed lowest value in the nine trees. The differences can be scaled up to 44% between the highest and the lowest groups based on the group mean values. Young's moduli showed the same order but opposite pattern due to the nature of $S_{LL} = E_L^{-1}$. In S_{RL}, SM1 showed highest value in magnitude, and YP2 the lowest, with 83% difference. In S_{TL}, SM1 and SM2 showed the same and highest values in the nine trees. They are significantly higher than YP2, WO1, and HM2.

Mean values of compliances, E_R, and ν_{RT} for trees that were loaded in compression in the R direction are shown in Table 23 for one type of gage installation (refer to Fig. 3A). In S_{RR}, COT1 had the highest compliance value, and WO1 the lowest. In between were YP2, SM2, RO2, SM1, YP1, RO1, and HM2. COT1, which was significantly higher in S_{RR} than WO1, yielded more than two-fold value to WO1. In S_{TR}, COT1 had significantly higher value than the rest of the trees, and the difference was up to about triple fold over WO1, one with the lowest value. The Young's moduli showed an opposite pattern to S_{RR}. In Poisson's ratios, trees exhibited clear grouping patterns. COT1 and HM2 were in the same group and ranked the highest, followed by SM2, SM1, and YP1 group, YP2 and WO1 were in the next group, followed by RO1, and finally, RO2, the lowest ranking.

The other results are listed in Table 24 for the gage settings shown in Fig. 3B. There was more than two-fold difference in S_{RR} within the nine trees. The order can be demonstrated as: COT1 > SM2 = RO2 = YP2 > SM1 = YP1 > HM2 = RO1 > WO1. In S_{LR}, the ranking pattern was different, with SM2 and COT1 in the highest group, and YP1 and HM2 in the lowest group. The Young's moduli indicated an opposite pattern to S_{RR}. For Poisson's ratios, RO1 and WO1 were in the same group and had the highest value. COT1, on the other hand, had the lowest value.

Mean values of compliances, E_T, and ν_{TR} for trees loaded in compression in the T direction are shown in Table 25 for the gage installation method displayed in Fig. 4A. In S_{TT}, COT1 ranked the highest, and displayed about a triple-fold higher value than RO1. Even the second-highest tree YP1 showed only about half of the value in COT1. In S_{RT}, the order can be demonstrated as COT1 > SM1 = SM2 = YP1 > YP2 > HM2 > RO2 > RO1 = WO1. Similarly, Young's moduli displayed an opposite pattern to S_{TT}. In Poisson's ratios, SM1, YP2, HM2, and SM2 fell in the same group and ranked the highest. On the other extreme, WO1 and COT1 fell in one group.

The other results are shown in Table 26 for the gage installation method displayed in Fig. 4B. COT1 exhibited a significantly higher S_{TT} value, about doubled the second highest value and tripled the lowest. The pattern can be displayed as a series of orders: COT1 > YP1 = SM2 = SM1 > RO2 = HM2 = YP2 > RO1 = WO1. In S_{LT}, SM1 showed highest value in term of magnitude, followed by SM2, COT1 and YP1 in the next group, followed by YP2, RO1, WO1 and RO2, and lastly HM2. The order of Young's moduli are opposite to S_{TT} due to $E_T = 1 / S_{TT}$. Poisson's ratios also showed variation among the nine trees tested, ranging from 0.0177 of COT1 to 0.0459 of SM1. The order can be displayed as SM1 > SM2 > RO1 > YP2 = WO1 > YP1 = RO2 = HM2 > COT1.

SUMMARY AND CONCLUSIONS

Strains parallel and perpendicular to the load axis were recorded for specimens from nine different hardwood trees representing six species loaded in the L, R, and T directions at moisture contents between 7% and 13%. Non-shear compliances in terms of strain in the L, R, and T directions per unit of stress in the loading direction (either L, R, or T) were calculated from this data. Conclusions were as follows:

1. Linear relationship were found between pairs of compliances: $S_{RL} = f(S_{LL})$, $S_{TL} = f(S_{LL})$, $S_{TR} = f(S_{RR})$, $S_{RT} = f(S_{TT})$, $S_{LR} = f(S_{RR})$, and $S_{LT} = f(S_{TT})$. The correlation factors R^2 for the first four equations were 0.566 or greater. However, R^2 for the last two equations were 0.332 and 0.100. In part this can be explained by the greater difficulty in measuring S_{LR} and S_{LT} than in measuring the other compliances.

2. With the exception of the relationship between S_{LT} and S_{TT}, slopes of equations from this report (Equation 2) relating pairs of non-shear compliances to each other were in general agreement with those in Equation 1 published

previously by Sliker (1985, 1988, and 1989). The slope of the equation with S_{LT} as a function of S_{TT} showed a significant difference from Sliker's equation (1989) at the 95% probability level.

3. Intercepts for the equations $S_{LR} = f(S_{RR})$ and $S_{LT} = f(S_{TT})$ were the only intercepts statistically significant at the 95% probability level. Dividing $S_{LR} = f(S_{RR})$ by S_{RR} and $S_{LT} = f(S_{TT})$ by S_{TT} provided equations for predicting the Poisson's ratios ν_{RL} and ν_{TL}.

4. The averaged values of Poisson's ratios obtained from current study are not significantly different from those reported by Sliker except the Poisson's ratio ν_{RL} that is significantly larger than that found by Sliker with 95% probability level (Table 9).

5. Trees studied in this experiment differed significantly in compliances and Young's modulus but did not show differences in Poisson's ratios when the specimens were loaded in compression in the L direction (Table 19).

6. Trees that were loaded in compression in either the R or T directions displayed significant differences in compliances and elastic constants investigated (Tables 20 and 21).

7. For this data S_{TR} very closely equaled S_{RT}. There was not sufficient data to test that $S_{RL} = S_{LR}$ and $S_{TL} = S_{LT}$.

8. Compliances and elastic constants that are not documented can be predicted for many wood species for use in finite element solutions to three dimensional stress and strain problems.

Table 1. Specific gravities and moisture contents measured for specimens made from nine test trees

Species[1]	Specific gravity at 0% MC[2]	Specific gravity at certain MC[3]	MC[4] (%)
Cottonwood (*Populus deltoides* S.) (COT1)	0.39	0.37	11.88
Yellow-poplar (*Liriodendron tulipifera* L.) (YP1)	0.46	0.45	10.22
Yellow-poplar (*Liriodendron tulipifera* L.) (YP2)	0.50	0.48	10.75
Soft maple (*Acer* species) (SM1)	0.53	0.50	12.25
Soft maple (*Acer* species) (SM2)	0.51	0.48	11.08
Red oak (*Quercus* species) (RO1)	0.66	0.64	10.84
Red oak (*Quercus* species) (RO2)	0.62	0.60	10.60
Hard maple (*Acer* species) (HM2)	0.65	0.61	11.06
White oak (*Quercus* species) (WO1)	0.72	0.69	11.52

[1]the numbers after the abbreviation of species represent trees.
[2]based on oven-dry weight and oven-dry volume.
[3]based on oven-dry weight and volume at time of specimen preparation.
[4]moisture content obtained at the time of specimen preparation.

Table 2. Compliances, Young's modulus, Poisson's ratios and moisture content for specimens loaded in the L direction and with lateral strain measured in the R and T directions

Species[1]	Specimen number	S_{LL} (1/psi) (1×10^{-6})	S_{RL} (1/psi) (1×10^{-6})	S_{TL} (1/psi) (1×10^{-6})	$E_L = 1/S_{LL}$ (psi) (1×10^{6})	$\nu_{LR} = \lvert \varepsilon_R/\varepsilon_L \rvert$	$\nu_{LT} = \lvert \varepsilon_T/\varepsilon_L \rvert$	MC[2] (%)
Cottonwood	COT1-L1	0.676	-0.228	-0.245	1.479	0.337	0.362	11.02
(COT1)	COT1-L2	0.820	-0.313	-0.355	1.220	0.382	0.433	11.02
Yellow-poplar	YP1-L1	0.600	-0.192	-0.252	1.667	0.320	0.420	11.00
(YP1)	YP1-L2	0.649	-0.236	-0.323	1.540	0.364	0.498	11.00
Yellow-poplar	YP2-L1	0.528	-0.162	-0.228	1.894	0.307	0.432	10.93
(YP2)	YP2-L2	0.499	-0.172	-0.246	2.004	0.345	0.493	10.97
Soft maple	SM1-L1	0.710	-0.309	-0.342	1.408	0.435	0.482	12.40
(SM1)	SM1-L2	0.704	-0.300	-0.351	1.420	0.426	0.499	12.40
Soft maple	SM2-L1	0.667	-0.291	-0.343	1.499	0.436	0.514	11.62
(SM2)	SM2-L2	0.649	-0.284	-0.350	1.540	0.438	0.539	11.62
Red oak	RO1-L1	0.629	-0.233	-0.295	1.590	0.370	0.469	11.02
(RO1)	RO1-L2	0.618	-0.231	-0.350	1.618	0.374	0.566	11.02
Red oak	RO2-L1	0.721	-0.218	-0.261	1.387	0.302	0.362	9.06
(RO2)	RO2-L2	0.731	-0.257	-0.286	1.368	0.352	0.391	9.06
Hard maple	HM2-L1	0.466	-0.213	-0.216	2.146	0.457	0.464	11.06
(HM2)	HM2-L2	0.490	-0.214	-0.239	2.041	0.437	0.488	11.01
White oak	WO1-L1	0.475	-0.173	-0.225	2.105	0.364	0.474	11.38
(WO1)	WO1-L2	0.498	-0.188	-0.208	2.008	0.378	0.418	11.38

[1] the numbers after the abbreviation of species represent trees.
[2] moisture content measured at the time of test.

Table 3. Comliances, Young's modulus, Poisson's ratio and moisture content for specimens loaded in the R direction and with lateral strain measured in the T direction

Species[1]	Specimen number	S_{RR} (1/psi) (1×10^{-6})	S_{TR} (1/psi) (1×10^{-6})	$E_R = 1/S_{RR}$ (psi)	$\nu_{RT} = \lvert \varepsilon_T/\varepsilon_R \rvert$	MC[2] (%)
Cottonwood	COT1-R2	7.53	-6.50	133,000	0.863	11.33
(COT1)	COT1-R3	7.71	-6.28	130,000	0.814	11.33
Yellow-poplar	YP1-R1	4.54	-3.38	220,000	0.744	10.38
(YP1)	YP1-R2	4.47	-3.27	224,000	0.732	10.38
Yellow-poplar	YP2-R1	5.11	-3.33	196,000	0.652	11.17
(YP2)	YP2-R2	5.15	-3.33	194,000	0.647	11.17
Soft maple	SM1-R1	4.57	-3.54	219,000	0.775	12.09
(SM1)	SM1-R2	4.81	-3.45	208,000	0.717	12.09
Soft maple	SM2-R1	5.09	-3.93	196,000	0.772	11.44
(SM2)	SM2-R2	5.08	-3.97	197,000	0.781	11.44
Red oak	RO1-R1	3.82	-2.30	262,000	0.602	9.98
(RO1)	RO1-R2	3.88	-2.25	258,000	0.580	9.98
Red oak	RO2-R1	4.91	-2.55	204,000	0.519	8.57
(RO2)	RO2-R2	4.88	-2.62	205,000	0.537	8.57
Hard maple	HM2-R1	3.75	-3.26	267,000	0.869	10.80
(HM2)	HM2-R2	3.84	-3.11	260,000	0.810	10.80
White oak	WO1-R1	3.45	-2.14	290,000	0.620	11.07
(WO1)	WO1-R2	3.66	-2.18	273,000	0.596	11.07

[1]the numbers after the abbreviation of species represent trees.
[2]moisture content measured at the time of test.

Table 4. Comliances, Young's modulus, Poisson's ratio and moisture content for specimens loaded in the R direction and with lateral strain measured in the L direction

Species[1]	Specimen number	S_{RR} (1/psi) (1 x 10^{-6})	S_{LR} (1/psi) (1 x 10^{-6})	E_R = 1/S_{RR} (psi)	ν_{RL} = $\lvert\varepsilon_L/\varepsilon_R\rvert$	MC^2(%)
Cottonwood	COT1-R1	7.49	-0.317	134,000	0.0423	11.33
(COT1)	COT1-R4	7.47	-0.305	134,000	0.0408	11.33
Yellow-poplar	YP1-R3	4.65	-0.258	215,000	0.0554	10.38
(YP1)	YP1-R4	4.68	-0.241	214,000	0.0515	10.38
Yellow-poplar	YP2-R3	5.01	-0.284	200,000	0.0567	11.17
(YP2)	YP2-R4	5.04	-0.273	198,000	0.0542	11.17
Soft maple	SM1-R3	4.65	-0.294	215,000	0.0632	12.09
(SM1)	SM1-R4	4.85	-0.283	206,000	0.0583	12.09
Soft maple	SM2-R3	4.96	-0.320	202,000	0.0645	11.44
(SM2)	SM2-R4	5.14	-0.330	195,000	0.0642	11.44
Red oak	RO1-R3	3.98	-0.292	251,000	0.0734	9.98
(RO1)	RO1-R4	3.87	-0.287	258,000	0.0742	9.98
Red oak	RO2-R3	5.05	-0.286	198,000	0.0566	8.57
(RO2)	RO2-R4	5.05	-0.264	198,000	0.0523	8.57
Hard maple	HM2-R3	4.13	-0.235	242,000	0.0569	10.80
(HM2)	HM2-R4	3.97	-0.241	252,000	0.0607	10.88
White oak	WO1-R3	3.53	-0.260	283,000	0.0737	11.10
(WO1)	WO1-R4	3.54	-0.256	282,000	0.0723	11.10

[1]the numbers after the abbreviation of species represent trees.
[2]moisture content measured at the time of test.

Table 5. Compliances, Young's modulus, Poisson's ratio and moisture content for specimens loaded in the T direction and with lateral strain measured in the R direction

Species[1]	Specimen number	S_{TT} (1/psi) (1 x 10^{-6})	S_{RT} (1/psi) (1 x 10^{-6})	$E_T = 1/S_{TT}$ (psi)	$\nu_{TR} = \lvert \varepsilon_R/\varepsilon_T \rvert$	MC^2 (%)
Cottonwood	COT1-T2	21.53	-6.18	46,400	0.287	11.34
(COT1)	COT1-T3	20.70	-6.32	48,300	0.305	11.34
Yellow-poplar	YP1-T1	10.88	-3.62	91,900	0.333	10.51
(YP1)	YP1-T2	11.47	-3.62	87,200	0.316	10.51
Yellow-poplar	YP2-T1	8.91	-3.14	112,000	0.352	11.19
(YP2)	YP2-T2	9.17	-3.13	109,000	0.341	11.19
Soft maple	SM1-T1	10.30	-3.63	97,100	0.352	12.07
(SM1)	SM1-T2	9.54	-3.64	105,000	0.382	12.07
Soft maple	SM2-T1	10.61	-3.53	94,300	0.333	11.54
(SM2)	SM2-T2	10.41	-3.60	96,100	0.346	11.54
Red oak	RO1-T1	7.33	-2.22	136,000	0.303	9.79
(RO1)	RO1-T2	7.47	-2.34	134,000	0.313	9.79
Red oak	RO2-T1	8.54	-2.44	117,000	0.286	7.82
(RO2)	RO2-T2	8.76	-2.32	114,000	0.265	7.82
Hard maple	HM2-T1	8.52	-2.96	117,000	0.347	10.92
(HM2)	HM2-T2	8.70	-2.96	115,000	0.340	10.92
White oak	WO1-T1	8.00	-2.17	125,000	0.271	11.09
(WO1)	WO1-T2	8.16	-2.20	123,000	0.270	11.09

[1]the numbers after the abbreviation of species represent trees.
[2]moisture content measured at the time of test.

Table 6. Compliances, Young's modulus, Poisson's ratio and moisture content for specimens loaded in the T direction and with lateral strain measured in the L direction

Species[1]	Specimen number	S_{TT} (1/psi) (1 x 10^{-6})	S_{LT} (1/psi) (1 x 10^{-6})	E_T = $1/S_{TT}$ (psi)	ν_{TL} = $\lvert\varepsilon_L/\varepsilon_T\rvert$	MC[2] (%)
Cottonwood	COT1-T1	19.82	-0.364	50,500	0.0184	11.27
(COT1)	COT1-T4	20.55	-0.348	48,700	0.0169	11.34
Yellow-poplar	YP1-T3	11.04	-0.345	90,600	0.0313	10.51
(YP1)	YP1-T4	10.30	-0.313	97,100	0.0304	10.51
Yellow-poplar	YP2-T3	8.98	-0.293	111,000	0.0326	11.19
(YP2)	YP2-T4	8.40	-0.301	119,000	0.0358	11.07
Soft maple	SM1-T3	9.91	-0.461	101,000	0.0465	12.07
(SM1)	SM1-T4	10.28	-0.465	97,300	0.0452	12.07
Soft maple	SM2-T3	10.38	-0.446	96,300	0.0430	11.54
(SM2)	SM2-T4	10.18	-0.404	98,200	0.0397	11.54
Red oak	RO1-T3	7.72	-0.289	130,000	0.0374	9.79
(RO1)	RO1-T4	7.83	-0.291	128,000	0.0372	9.79
Red oak	RO2-T3	9.07	-0.265	110,000	0.0292	7.82
(RO2)	RO2-T4	9.35	-0.276	107,000	0.0295	7.82
Hard maple	HM2-T3	9.00	-0.271	111,000	0.0301	10.92
(HM2)	HM2-T4	8.95	-0.253	112,000	0.0283	10.92
White oak	WO1-T3	7.90	-0.266	127,000	0.0337	11.10
(WO1)	WO1-T4	7.62	-0.264	131,000	0.0346	11.10

[1]the numbers after the abbreviation of species represent trees.
[2]moisture content measured at the time of test.

Table 7. Statistical analysis of slopes between the current data and Sliker's data for compliance equations

Equation	Sliker's data (1985, 1988, 1989)			This report data			t	$t_{0.05}$
	Slope	Std. dev.	n	Slope	Std. dev.	n		
$S_{RL} = f(S_{LL})$	-0.405	0.144	18	-0.353	0.318	9	0.59	2.060
$S_{TL} = f(S_{LL})$	-0.500	0.153	18	-0.360	0.357	9	1.44	2.060
$S_{TR} = f(S_{RR})$	-0.887	0.302	11	-0.967	0.447	9	0.48	2.101
$S_{LR} = f(S_{RR})$	-0.0483	0.044	10	-0.0143	0.0231	9	2.00	2.110
$S_{RT} = f(S_{TT})$	-0.255	0.042	9	-0.288	0.0855	9	1.03	2.120
$S_{LT} = f(S_{TT})$	-0.0274	0.0048	8	-0.00605	0.0204	9	3.05	2.262

Table 8. Statistics of slopes and intercepts for compliance equations

Equation	Slope			Intercept		
	Standard Error	T value	Pr > T	Standard Error	T value	Pr > T
1. $S_{RL} = -0.016 \times 10^{-6} - 0.353\ S_{LL}$	0.1061	-3.330	0.0126	0.0664	-0.241	0.8163
2. $S_{TL} = -0.062 \times 10^{-6} - 0.360\ S_{LL}$	0.1192	-3.022	0.0193	0.0747	-0.826	0.4358
3. $S_{TR} = 1.224 \times 10^{-6} - 0.967\ S_{RR}$	0.1489	-6.498	0.0003	0.7332	1.670	0.1389
4. $S_{LR} = -0.210 \times 10^{-6} - 0.0143\ S_{RR}$	0.0077	-1.866	0.1043	0.0380	-5.539	0.0009
5. $S_{RT} = -\ 0.309 \times 10^{-6} - 0.288\ S_{TT}$	0.0285	-10.111	0.0001	0.3194	-0.968	0.3654
6. $S_{LT} = -0.266 \times 10^{-6} - 0.00605\ S_{TT}$	0.0068	-0.883	0.4066	0.0754	-3.525	0.0097

Table 9. Statistical analysis of Poisson's ratios between the current data and Sliker's data

Poisson's ratios	Sliker's data (1985, 1988, 1989)			This report data			t	$t_{0.05}$
	Mean	Std. dev.	n	Mean	Std. dev.	n		
ν_{LR}	0.373	0.0392	18	0.379	0.0487	18	0.40	2.031
ν_{LT}	0.469	0.0422	18	0.461	0.0568	18	0.78	2.031
ν_{RT}	0.642	0.1261	12	0.702	0.1102	18	1.38	2.048
ν_{RL}	0.043	0.0114	10	0.060	0.0099	18	4.36	2.056
ν_{TR}	0.332	0.0616	10	0.319	0.0336	18	0.72	2.056
ν_{TL}	0.030	0.0040	8	0.033	0.0079	18	0.11	2.064

Table 10. Estimates of the variability among individual observations for compliance S_{RR}

Species[1]	Number of specimens	S_{RR}[2] Mean (1/psi) (1×10^{-6})	S_{RR}[2] Std. dev. (1/psi) (1×10^{-6})	S_{RR}[2] CV (%)	S_{RR}[3] Mean (1/psi) (1×10^{-6})	S_{RR}[3] Std. dev. (1/psi) (1×10^{-6})	S_{RR}[3] CV (%)
COT1	2	7.620	0.1273	1.67	7.480	0.0141	0.19
YP1	2	4.505	0.0495	1.10	4.665	0.0212	0.45
YP2	2	5.130	0.0283	0.55	5.025	0.0212	0.42
SM1	2	4.690	0.1697	3.62	4.750	0.1414	2.98
SM2	2	5.085	0.0071	0.14	5.050	0.1273	2.52
RO1	2	3.850	0.0424	1.10	3.925	0.0778	1.98
RO2	2	4.895	0.0212	0.43	5.050	0	0
HM2	2	3.795	0.0636	1.68	4.050	0.1131	2.79
WO1	2	3.555	0.1485	4.18	3.535	0.0071	0.20

[1]the numbers after the abbreviation of species represent trees.
[2]gage installation shown in figure 3A.
[3]gage installation shown in figure 3B.

Table 11. Estimates of the variability among individual observations for compliance S_{TT}

Species[1]	Number of specimens	S_{TT}[2] Mean (1/psi) (1×10^{-6})	S_{TT}[2] Std. dev. (1/psi) (1×10^{-6})	S_{TT}[2] CV (%)	S_{TT}[3] Mean (1/psi) (1×10^{-6})	S_{TT}[3] Std. dev. (1/psi) (1×10^{-6})	S_{TT}[3] CV (%)
COT1	2	21.115	0.5869	2.78	20.185	0.5162	2.56
YP1	2	11.175	0.4172	3.73	10.670	0.5233	4.90
YP2	2	9.040	0.1838	2.03	8.690	0.4101	4.72
SM1	2	9.920	0.5374	5.42	10.095	0.2616	2.59
SM2	2	10.510	0.1414	1.35	10.280	0.1414	1.38
RO1	2	7.400	0.0990	1.34	7.775	0.0778	1.00
RO2	2	8.650	0.1556	1.80	9.210	0.1980	2.15
HM2	2	8.610	0.1273	1.48	8.975	0.0354	0.39
WO1	2	8.080	0.1131	1.40	7.760	0.1979	2.55

[1]the numbers after the abbreviation of species represent trees.
[2]gage installation shown in figure 4A.
[3]gage installation shown in figure 4B.

Table 12. Estimates of the variability among individual observations for compliance S_{LL}

Species*	Number of specimens	S_{LL} Mean (1/psi) (1×10^{-6})	Std. dev. (1/psi) (1×10^{-6})	CV (%)
COT1	2	0.748	0.1018	13.61
YP1	2	0.625	0.0346	5.55
YP2	2	0.514	0.0205	3.99
SM1	2	0.707	0.0042	0.60
SM2	2	0.658	0.0127	1.93
RO1	2	0.624	0.0078	1.25
RO2	2	0.726	0.0071	0.97
HM2	2	0.478	0.0170	3.55
WO1	2	0.487	0.0163	3.34

*the numbers after the abbreviation of species represent trees.

Table 13. Estimates of the variability among individual observations for compliance S_{RL}

Species*	Number of specimens	S_{RL} Mean (1/psi) (1×10^{-6})	Std. dev. (1/psi) (1×10^{-6})	CV (%)
COT1	2	-0.271	0.0601	22.22
YP1	2	-0.214	0.0311	14.54
YP2	2	-0.167	0.0071	4.23
SM1	2	-0.305	0.0064	2.09
SM2	2	-0.228	0.0049	1.72
RO1	2	-0.232	0.0014	0.61
RO2	2	-0.238	0.0276	11.61
HM2	2	-0.214	0.0007	0.33
WO1	2	-0.181	0.0106	5.88

*the numbers after the abbreviation of species represent trees.

Table 14. Estimates of the variability among individual observations for compliance S_{TL}

Species*	Number of specimens	S_{TL} Mean (1/psi) (1×10^{-6})	Std. dev. (1/psi) (1×10^{-6})	CV (%)
COT1	2	-0.300	0.0778	25.93
YP1	2	-0.288	0.0502	17.46
YP2	2	-0.237	0.0127	5.37
SM1	2	-0.347	0.0064	1.84
SM2	2	-0.347	0.0049	1.43
RO1	2	-0.323	0.0389	12.06
RO2	2	-0.274	0.0177	6.46
HM2	2	-0.228	0.0163	7.15
WO1	2	-0.217	0.0120	5.55

*the numbers after the abbreviation of species represent trees.

Table 15. Estimates of the variability among individual observations for compliance S_{TR}

Species*	Number of specimens	S_{TR} Mean (1/psi) (1×10^{-6})	Std. dev. (1/psi) (1×10^{-6})	CV (%)
COT1	2	-6.390	0.1556	2.43
YP1	2	-3.325	0.0778	2.34
YP2	2	-3.330	0	0
SM1	2	-3.495	0.0636	1.82
SM2	2	-3.950	0.0283	0.72
RO1	2	-2.275	0.0354	1.55
RO2	2	-2.585	0.0495	1.91
HM2	2	-3.185	0.1061	3.33
WO1	2	-2.160	0.0283	1.31

*the numbers after the abbreviation of species represent trees.

Table 16. Estimates of the variability among individual observations for compliance S_{LR}

Species*	Number of specimens	S_{LR} Mean (1/psi) (1×10^{-6})	Std. dev. (1/psi) (1×10^{-6})	CV (%)
COT1	2	-0.311	0.0085	2.73
YP1	2	-0.250	0.0120	4.82
YP2	2	-0.279	0.0078	2.79
SM1	2	-0.289	0.0078	2.70
SM2	2	-0.325	0.0071	2.18
RO1	2	-0.290	0.0035	1.22
RO2	2	-0.275	0.0156	5.66
HM2	2	-0.238	0.0042	1.78
WO1	2	-0.258	0.0028	1.10

*the numbers after the abbreviation of species represent trees.

Table 17. Estimates of the variability among individual observations for compliance S_{RT}

Species*	Number of specimens	S_{RT} Mean (1/psi) (1×10^{-6})	S_{RT} Std. dev. (1/psi) (1×10^{-6})	S_{RT} CV (%)
COT1	2	-6.250	0.0990	1.58
YP1	2	-3.620	0	0
YP2	2	-3.135	0.0071	0.23
SM1	2	-3.635	0.0071	0.19
SM2	2	-3.565	0.0495	1.39
RO1	2	-2.280	0.0849	3.72
RO2	2	-2.380	0.0849	3.57
HM2	2	-2.960	0	0
WO1	2	-2.185	0.0212	0.97

*the numbers after the abbreviation of species represent trees.

Table 18. Estimates of the variability among individual observations for compliance S_{LT}

Species*	Number of specimens	S_{LT} Mean (1/psi) (1×10^{-6})	Std. dev. (1/psi) (1×10^{-6})	CV (%)
COT1	2	-0.356	0.0113	3.18
YP1	2	-0.329	0.0226	6.88
YP2	2	-0.297	0.0057	1.90
SM1	2	-0.463	0.0028	0.61
SM2	2	-0.425	0.0297	6.99
RO1	2	-0.290	0.0014	0.49
RO2	2	-0.271	0.0078	2.88
HM2	2	-0.262	0.0127	4.86
WO1	2	-0.265	0.0014	0.53

*the numbers after the abbreviation of species represent trees.

Table 19. Summary of analysis of variance over the differences among trees loaded in compression in the L direction

Parameter	Number of trees tested	n	F value	Pr > F
S_{LL}	9	18	15.07	0.0002
S_{RL}	9	18	7.01	0.0043
S_{TL}	9	18	4.00	0.0269
E_L	9	18	26.21	0.0001
ν_{LR}	9	18	2.72	0.0774
ν_{LT}	9	18	3.03	0.0597

Table 20. Summary of analysis of variance over the differences among trees loaded in compression in the R direction

Parameter	Number of trees tested	n	F value	Pr > F
S_{RR}[1]	9	18	343.81	0.0001
S_{TR}	9	18	565.26	0.0001
E_R[1]	9	18	147.22	0.0001
ν_{RT}	9	18	41.57	0.0001
S_{RR}[2]	9	18	412.17	0.0001
S_{LR}	9	18	21.38	0.0001
E_R[2]	9	18	233.38	0.0001
ν_{RL}	9	18	43.90	0.0001

[1]gage installation displayed in Fig. 3A.
[2]gage installation displayed in Fig. 3B.

Table 21. Summary of analysis of variance over the differences among trees loaded in compression in the T direction

Parameter	Number of trees tested	n	F value	Pr > F
S_{TT}[1]	9	18	336.16	0.0001
S_{RT}	9	18	1013.29	0.0001
E_T[1]	9	18	192.21	0.0001
ν_{TR}	9	18	16.93	0.0001
S_{TT}[2]	9	18	296.12	0.0001
S_{LT}	9	18	53.41	0.0001
E_T[2]	9	18	131.39	0.0001
ν_{TL}	9	18	78.32	0.0001

[1]gage installation displayed in Fig. 4A.
[2]gage installation displayed in Fig. 4B.

Table 22. Duncan's t-test over the means in compliances and Young's modulus for specimens loaded in the L direction and with lateral strain measured in the R and T directions

Species*	S_{LL} (1/psi) (1×10^{-6})	S_{RL} (1/psi) (1×10^{-6})	S_{TL} (1/psi) (1×10^{-6})	E_L (psi)
COT1	0.748a	-0.271abc	-0.300abc	1.350c
RO2	0.726a	-0.238bcd	-0.274abc	1.378c
SM1	0.707ab	-0.305a	-0.347a	1.414dc
SM2	0.658ab	-0.288ab	-0.347a	1.520bc
YP1	0.625b	-0.214cde	-0.288abc	1.604b
RO1	0.624b	-0.232bcd	-0.323ab	1.604b
YP2	0.514c	-0.167e	-0.237bc	1.949a
WO1	0.487c	-0.181de	-0.217c	2.057a
HM2	0.478c	-0.214cde	-0.228c	2.094a

*the numbers after the abbreviation of species represent trees.
Means in different letters within the same column are significantly different from each other at 95% probability level with Duncan's multiple range test.

Table 23. Duncan's t-test over the means in compliances Young's modulus and Poisson's ratio for specimens loaded in the R direction and with lateral strain measured in the T direction

Species*	S_{RR} (1/psi) (1×10^{-6})	S_{TR} (1/psi) (1×10^{-6})	E_R (psi)	ν_{RT}
COT1	7.620a	-6.390a	131500f	0.839a
YP2	5.130b	-3.330cd	195000e	0.650c
SM2	5.085bc	-3.950b	196500e	0.777b
RO2	4.895cd	-2.585e	204500de	0.528e
SM1	4.690de	-3.495c	213500cd	0.746b
YP1	4.505e	-3.325cd	222000c	0.738b
RO1	3.850f	-2.275f	260000b	0.591d
HM2	3.795f	-3.185d	263500b	0.840a
WO1	3.555g	-2.160f	281500a	0.608cd

*the numbers after the abbreviation of species represent trees.

Means in different letters within the same column are significantly different from each other at 95% probability level with Duncan's multiple range test.

Table 24. Duncan's t-test over the means in compliances Young's modulus and Poisson's ratio for specimens loaded in the R direction and with lateral strain measured in the L direction

Species*	S_{RR} (1/psi) (1×10^{-6})	S_{LR} (1/psi) (1×10^{-6})	E_R (psi)	ν_{RL}
COT1	7.480a	-0.311a	134000e	0.0416f
SM2	5.050b	-0.325a	198500d	0.0644b
RO2	5.050b	-0.275bc	198000d	0.0545de
YP2	5.025b	-0.279b	199000d	0.0555de
SM1	4.750c	-0.289b	210500c	0.0608bc
YP1	4.665c	-0.250d	214500c	0.0535e
HM2	4.050d	-0.238d	247000b	0.0588cd
RO1	3.925d	-0.290b	254500b	0.0738a
WO1	3.535e	-0.258cd	282500a	0.0730a

*the numbers after the abbreviation of species represent trees.

Means in different letters within the same column are significantly different from each other at 95% probability level with Duncan's multiple range test.

Table 25. Duncan's t-test over the means in compliances Young's modulus and Poisson's ratio for specimens loaded in the T direction and with lateral strain measured in the R direction

Species*	S_{TT} (1/psi) (1×10^{-6})	S_{RT} (1/psi) (1×10^{-6})	E_T (psi)	ν_{TR}
COT1	21.115a	-6.250a	47350f	0.296de
YP1	11.175b	-3.620b	89550e	0.325bc
SM2	10.510bc	-3.565b	95200de	0.340ab
SM1	9.920c	-3.635b	101050d	0.367a
YP2	9.040d	-3.135c	110500c	0.347ab
RO2	8.650de	-2.380e	115000c	0.276e
HM2	8.610de	-2.960d	116000c	0.344ab
WO1	8.080ef	-2.185f	124000b	0.271e
RO1	7.400f	-2.280f	135000a	0.308cd

*the numbers after the abbreviation of species represent trees.

Means in different letters within the same column are significantly different from each other at 95% probability level with Duncan's multiple range test.

Table 26. Duncan's t-test over the means in compliances Young's modulus and Poisson's ratio for specimens loaded in the T direction and with lateral strain measured in the L direction

Species*	S_{TT} (1/psi) (1×10^{-6})	S_{LT} (1/psi) (1×10^{-6})	E_T (psi)	ν_{TL}
COT1	20.185a	-0.356c	49600d	0.0177f
YP1	10.670b	-0.329c	93850c	0.0309e
SM2	10.280b	-0.425b	97250c	0.0414b
SM1	10.095b	-0.463a	99150c	0.0459a
RO2	9.210c	-0.271de	108500b	0.0294e
HM2	8.975c	-0.262e	111500b	0.0292e
YP2	8.690c	-0.297d	115000b	0.0342d
RO1	7.775d	-0.290de	129000a	0.0373c
WO1	7.760d	-0.265de	129000a	0.0342d

*the numbers after the abbreviation of species represent trees.
Means in different letters within the same column are significantly different from each other at 95% probability level with Duncan's multiple range test.

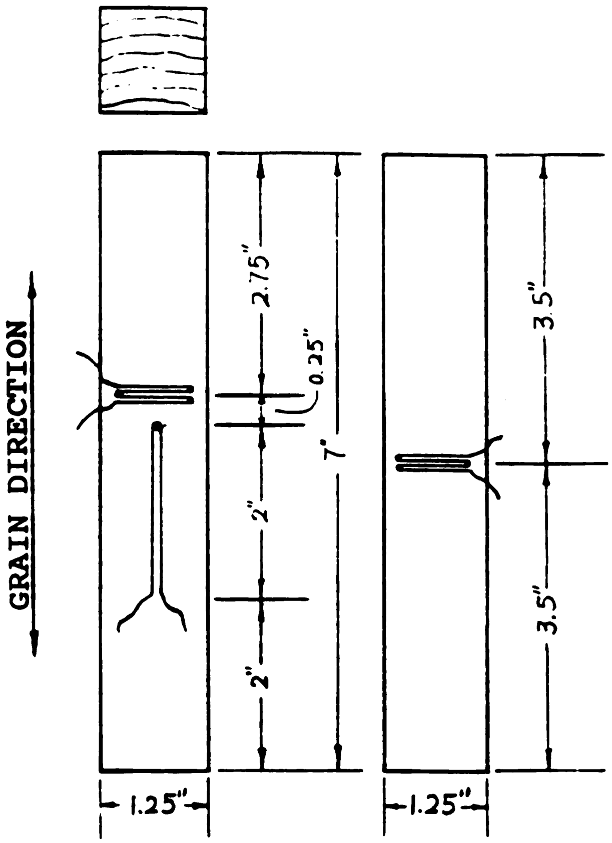

Figure 1. Compression parallel to grain samples with bonded wire strain gages for measuring strains parallel and perpendicular to the load axis (Sliker, 1985).

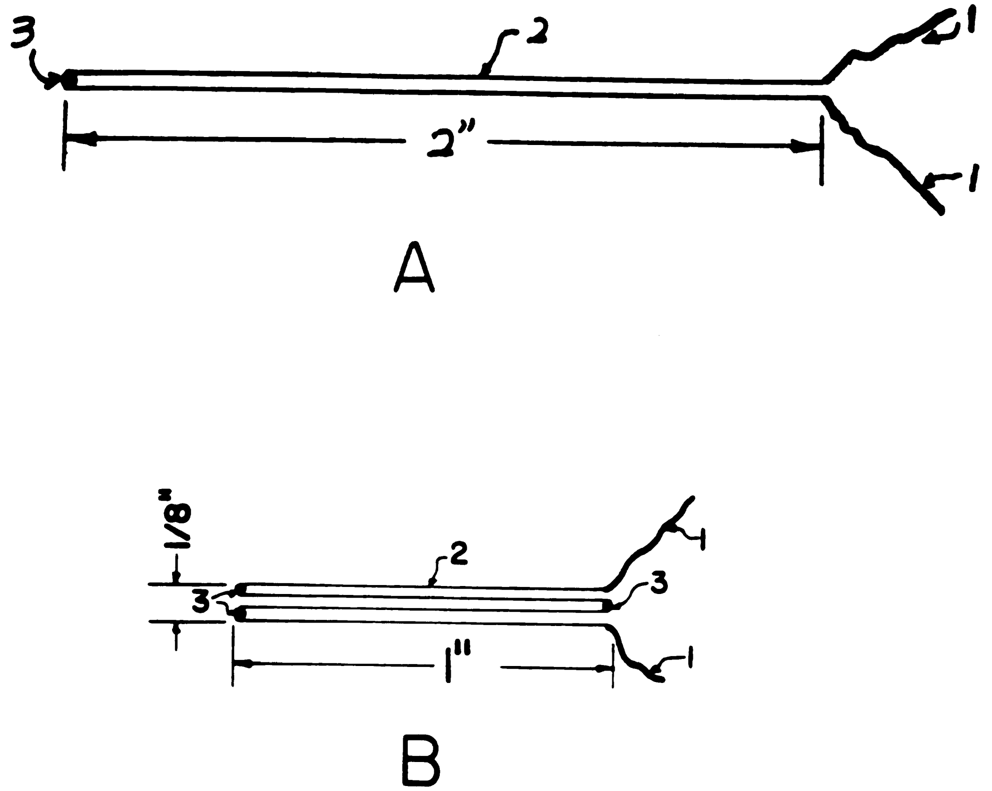

Figure 2. Gage type A used to measure strain in the L direction; gage type B used to measure strain in the R and T directions. 12-mil diameter constantan lead wires are indicated by the number 1; 1-mil diameter constantan wires for measuring strain are indicated by the number 2; straight pins around which strain wire is looped are indicated by the number 3 (Sliker, 1989).

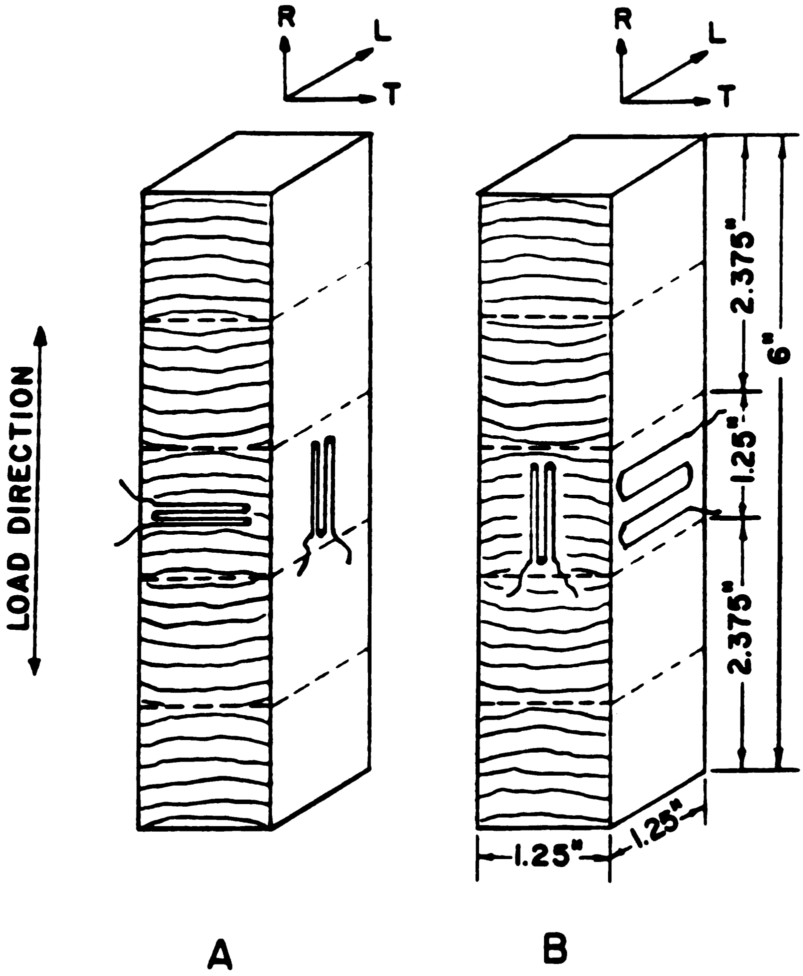

Figure 3. Specimens for loading in the R direction. In specimen A, the gage measuring strain in the R direction is on the radial surface and the gage measuring strain in the T direction is on the cross-section. In specimen B, the gage measuring strain in the R direction is on the cross-section and the gage measuring strain in the L direction is on the radial surface.

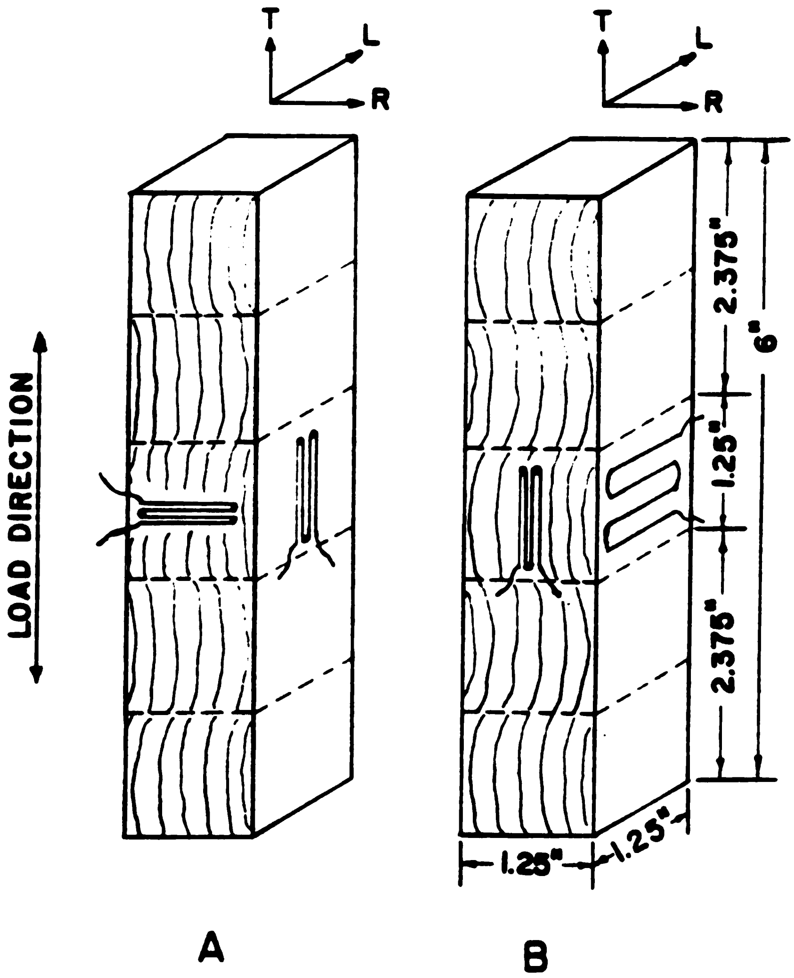

Figure 4. Specimens for loading in the T direction. In specimen A, the gage measuring strain in the T direction is on the tangential surface and the gage measuring strain in the R direction is on the cross-section. In specimen B, the gage measuring strain in the T direction is on the cross-section and the gage measuring strain in the L direction is on the tangential surface.

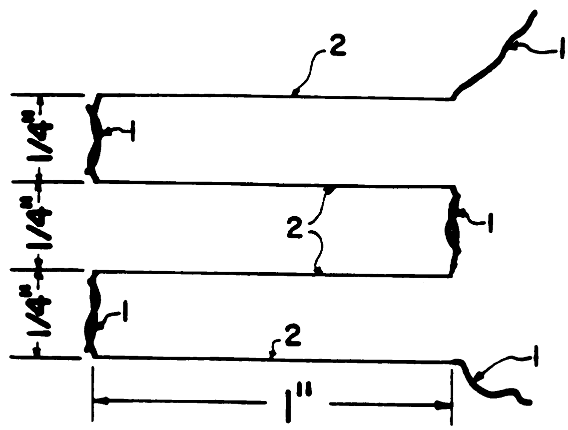

Figure 5. Gage type used to measure small strain in the L direction when specimens are loaded in the R or T direction. 12-mil diameter constantan lead wires are indicated by the number 1; 1-mil diameter constantan wires for measuring strain are indicated by the number 2 (Sliker, 1989).

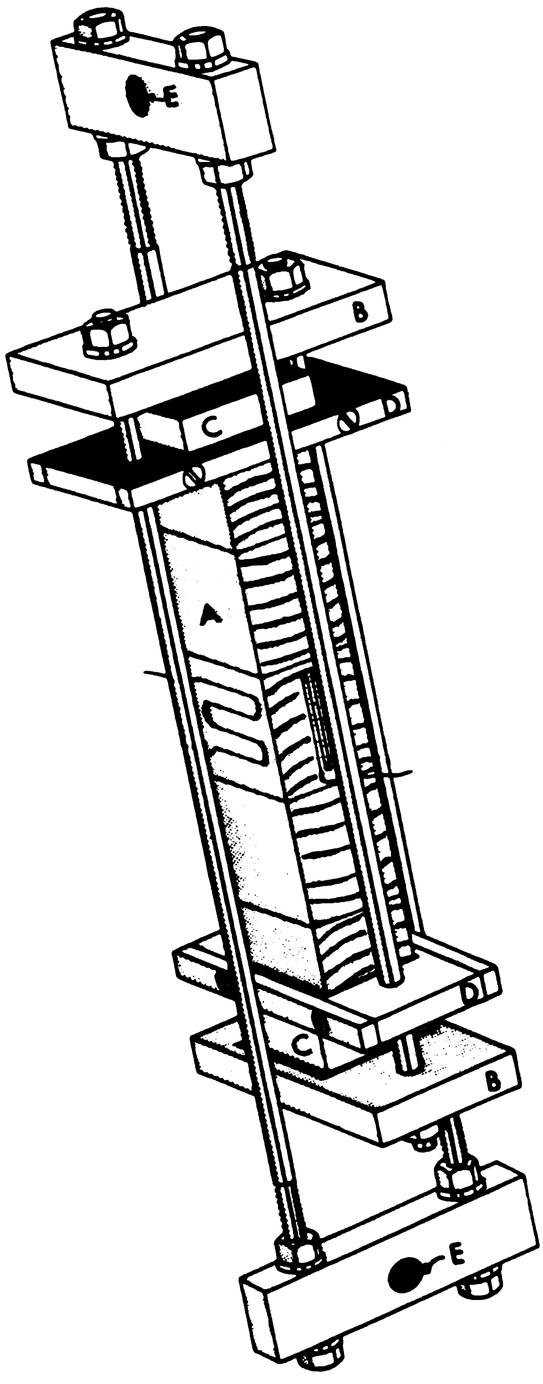

Figure 6. Test specimen A in the compression cage. B is end block. C is end bearing block. D is centering guide. E is hole for metal dowel connection to universal joint. Ball bearing is centered between B and C at each end (Sliker, 1989).

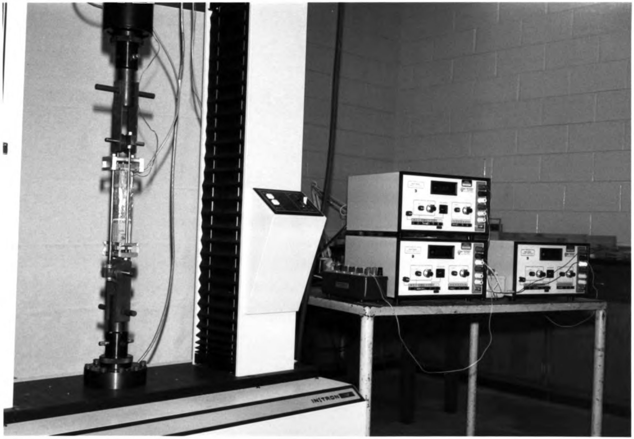

Figure 7. Specimen with long axis in the L direction being loaded in Instron testing machine (Sliker et al., in press).

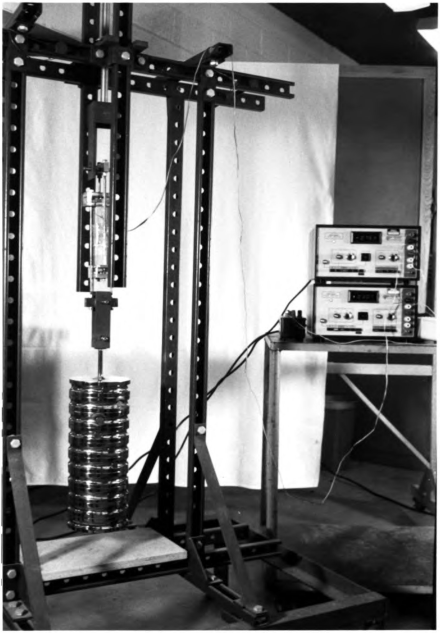

Figure 8. Specimen being loaded in either the R or T direction by application of ten 10-pound weights to a load hanger (Sliker et al., in press).

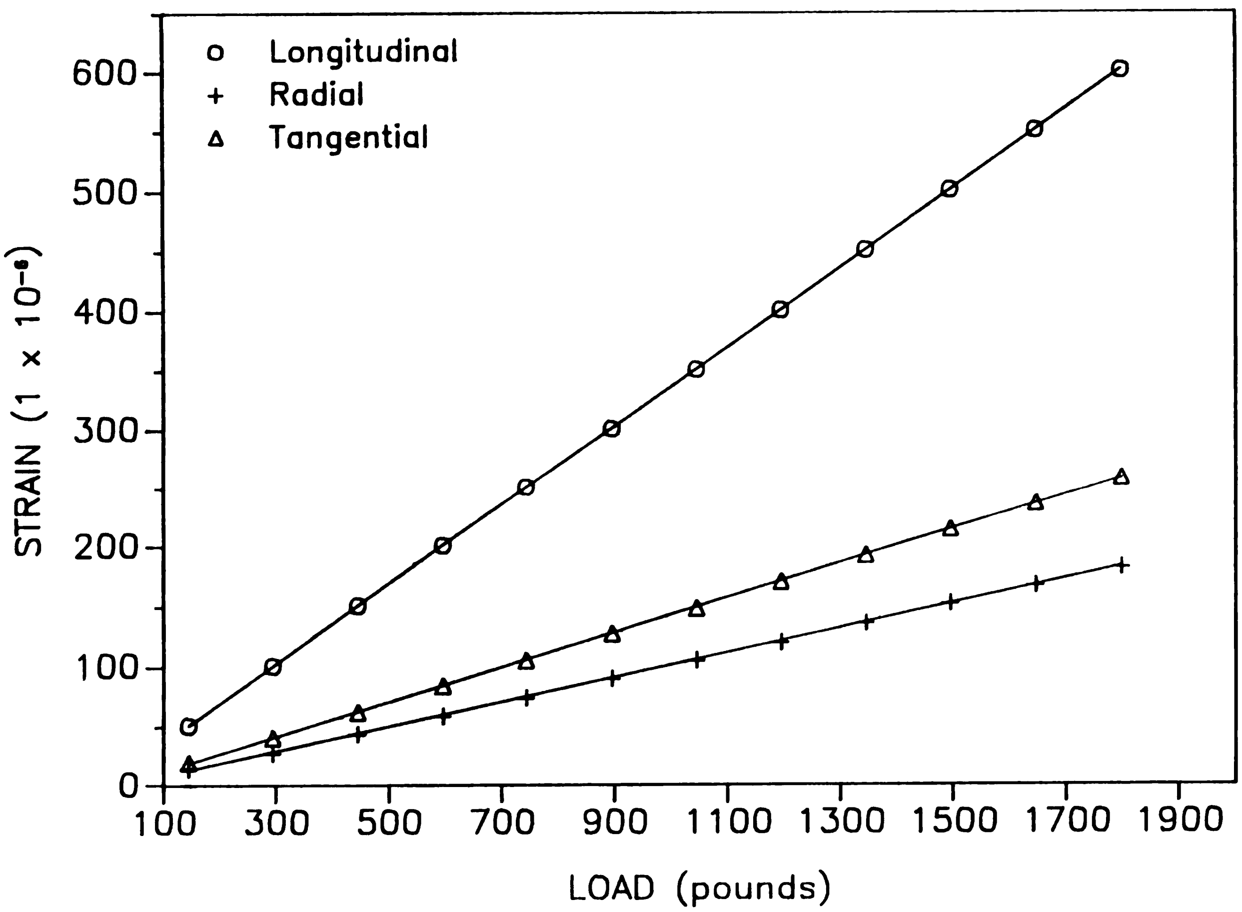

Figure 9. Plots of the strains in the L, R, and T directions versus compressive load applied in the L direction for yellow-poplar specimen YP2-1L. Strain in the L direction is negative while that in the R and T directions is positive.

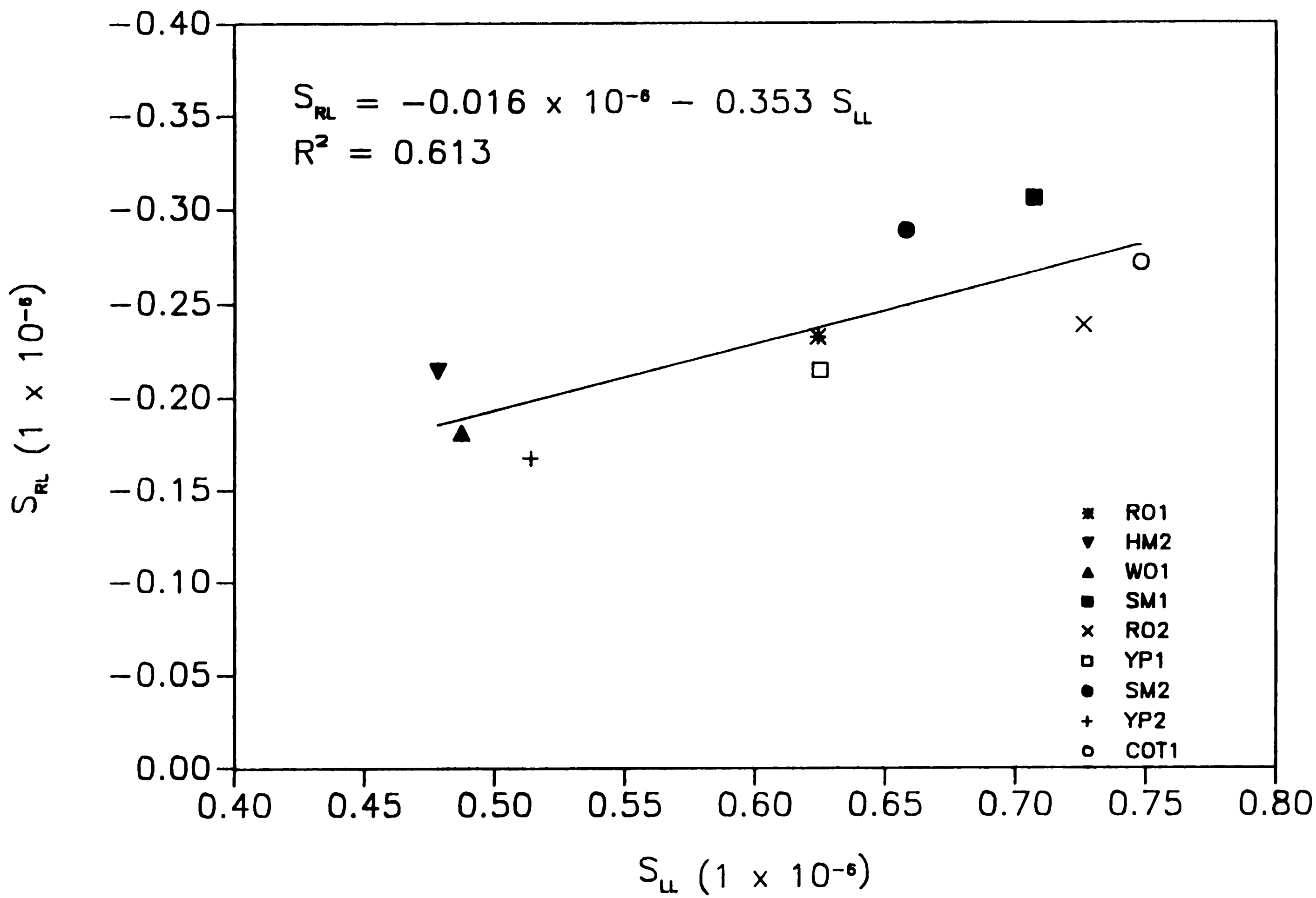

Figure 10. Compliance S_{RL} plotted as a function of compliance S_{LL} for specimen from nine trees loaded in the L direction. Each point is the average reading from two matched samples.

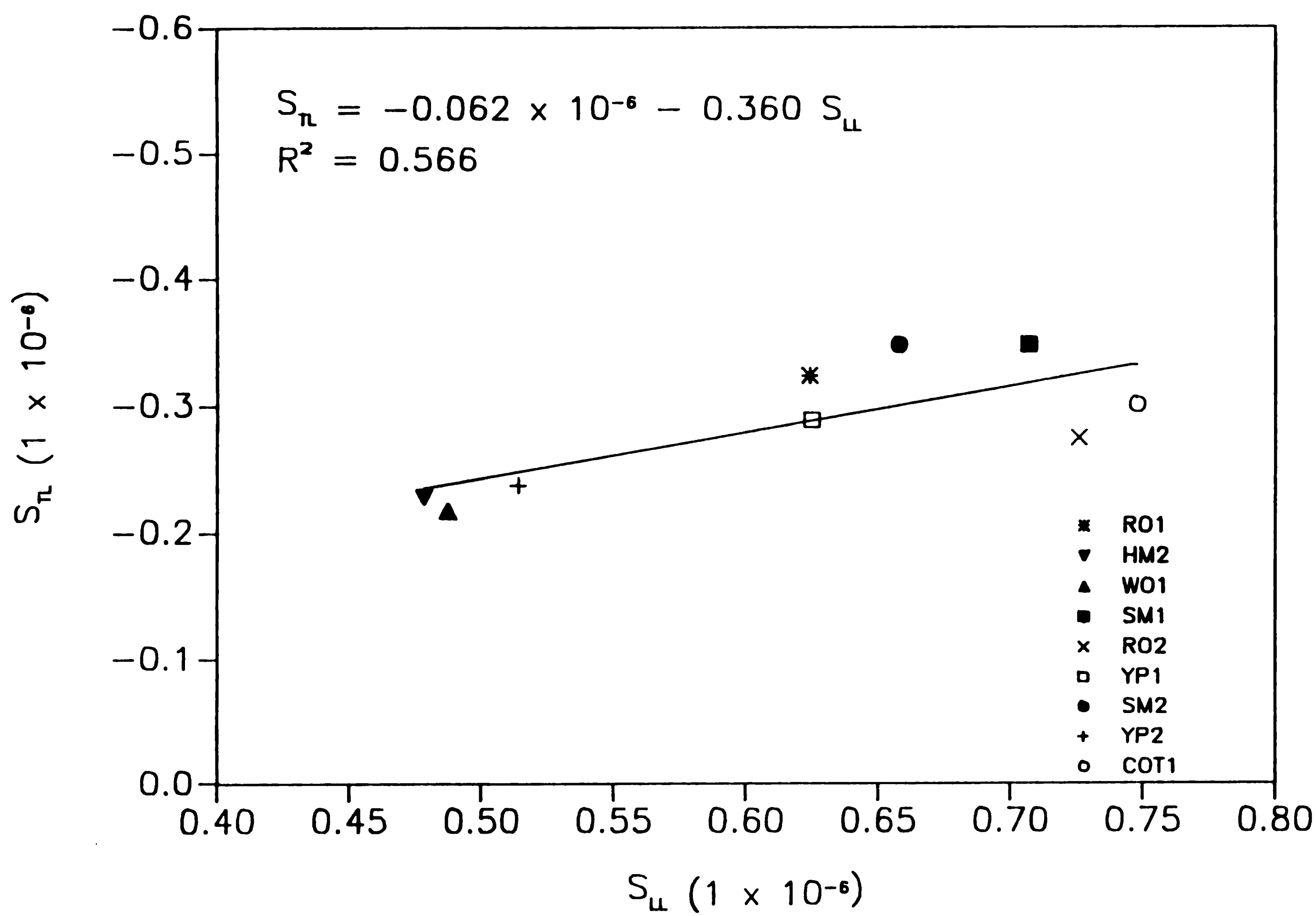

Figure 11. Compliance S_{TL} plotted as a function of compliance S_{LL} for specimen from nine trees loaded in the L direction. Each point is the average reading from two matched samples.

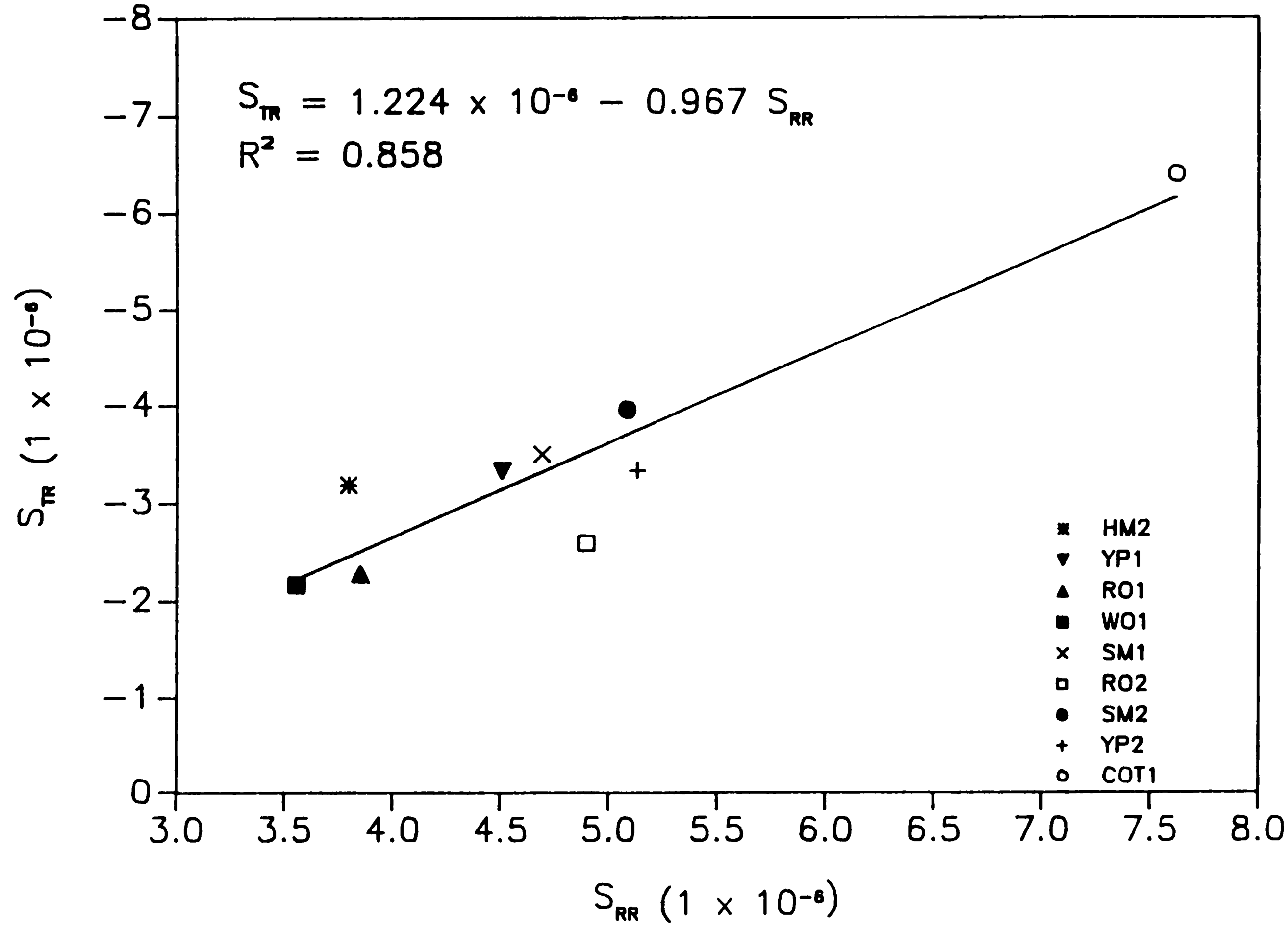

Figure 12. Compliance S_{TR} plotted as a function of compliance S_{RR} for specimen from nine trees loaded in the R direction. Each point is the average reading from two matched samples.

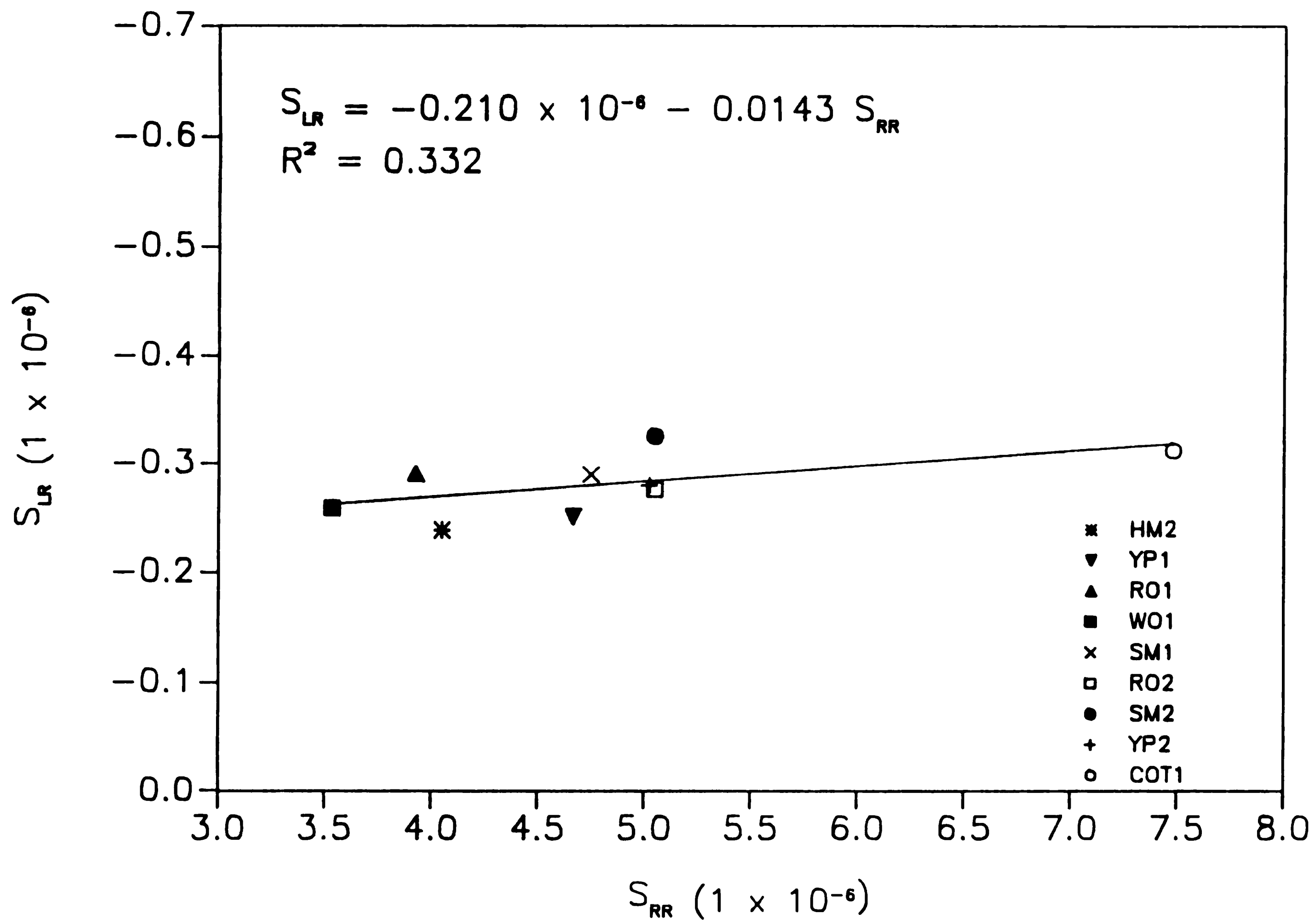

Figure 13. Compliance S_{LR} plotted as a function of compliance S_{RR} for specimen from nine trees loaded in the R direction. Each point is the average reading from two matched samples.

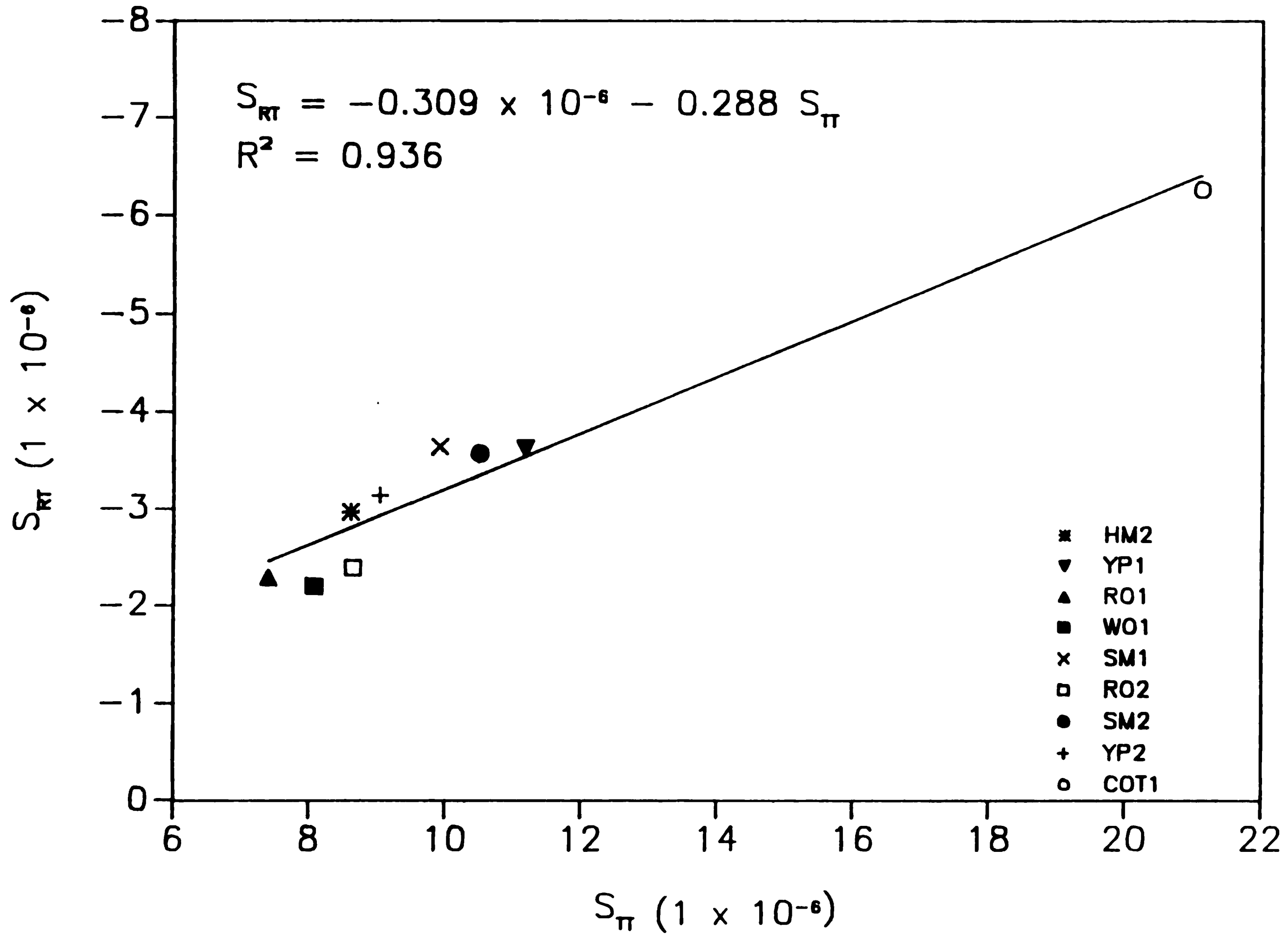

Figure 14. Compliance S_{RT} plotted as a function of compliance S_{TT} for specimen from nine trees loaded in the T direction. Each point is the average reading from two matched samples.

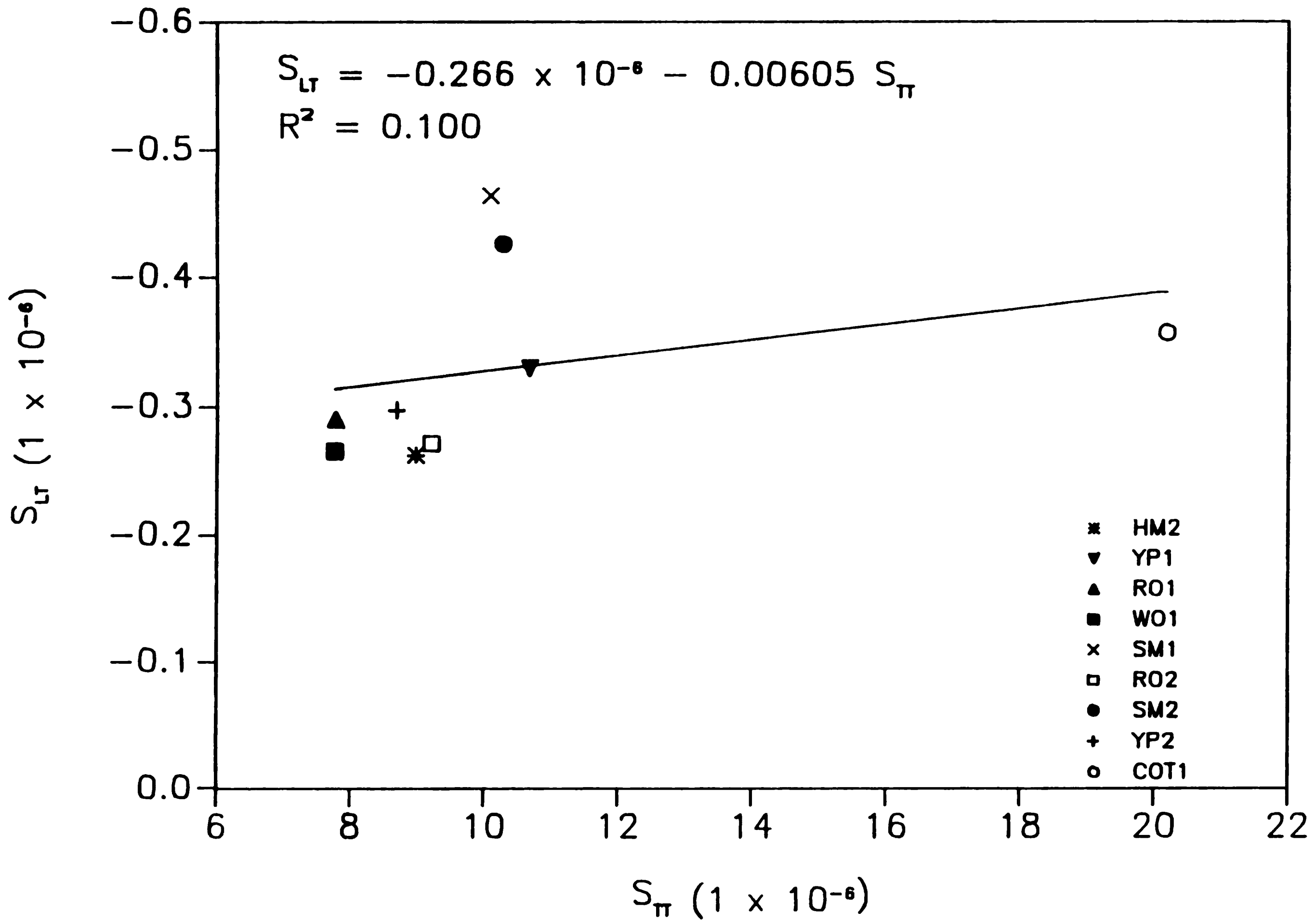

Figure 15. Compliance S_{LT} plotted as a function of compliance S_{TT} for specimen from nine trees loaded in the T direction. Each point is the average reading from two matched samples.

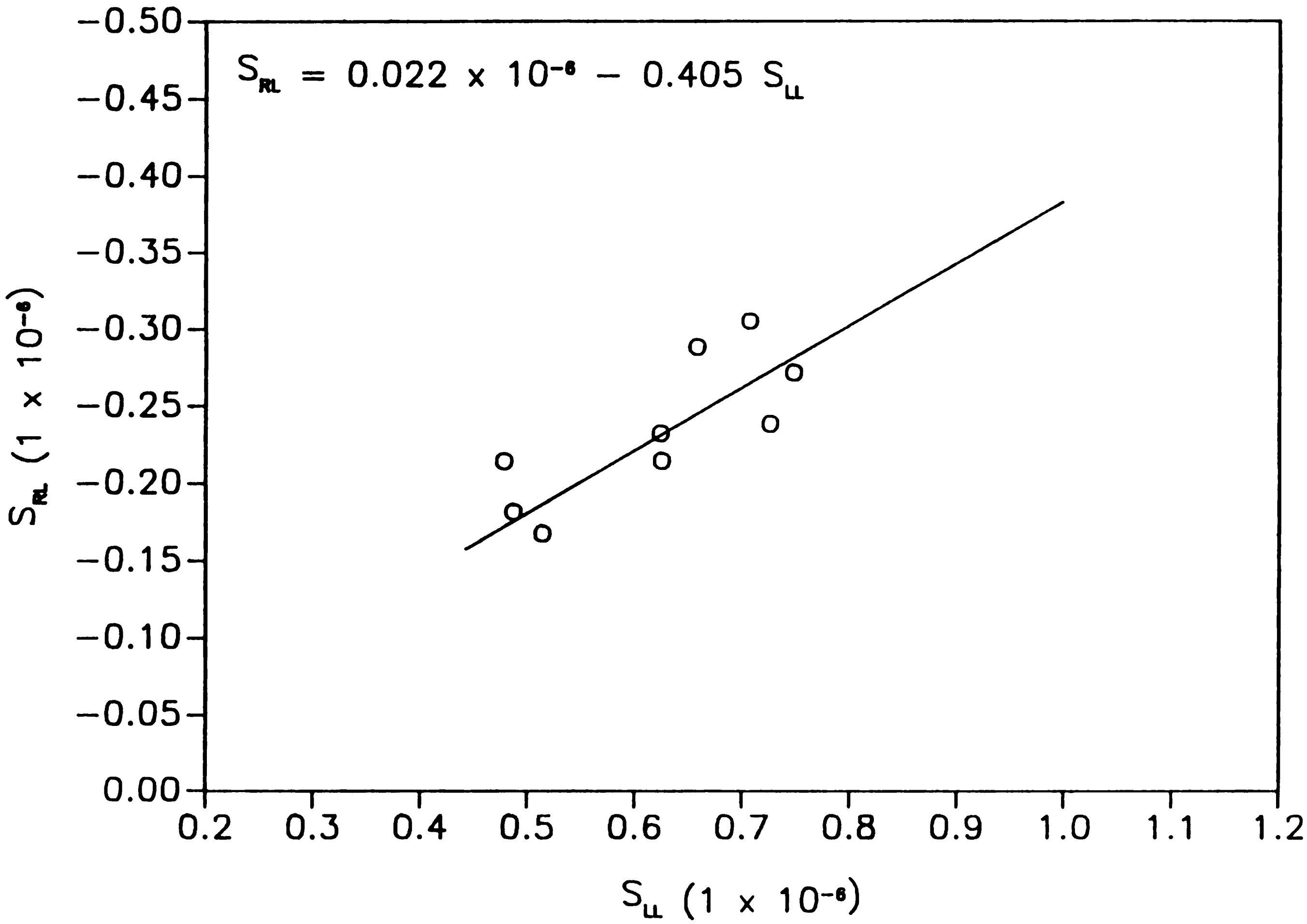

Figure 16. Plotted points showing the relationship between S_{RL} and S_{LL} from this study. The equation derived from Sliker (1985) expressing the relationship between the same two quantities is shown as the solid straight line.

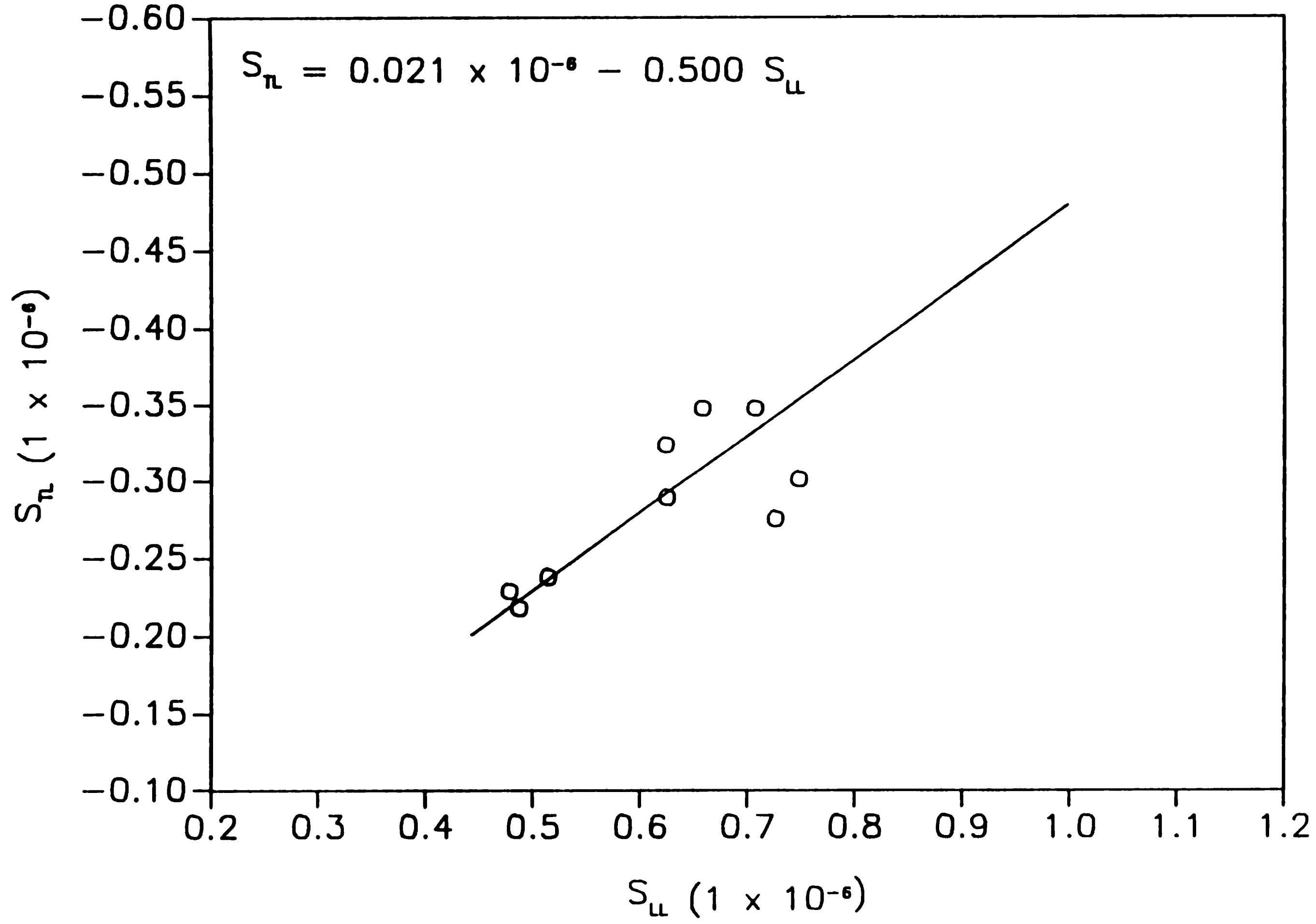

Figure 17. Plotted points showing the relationship between S_{TL} and S_{LL} from this study. The equation derived from Sliker (1985) expressing the relationship between the same two quantities is shown as the solid straight line.

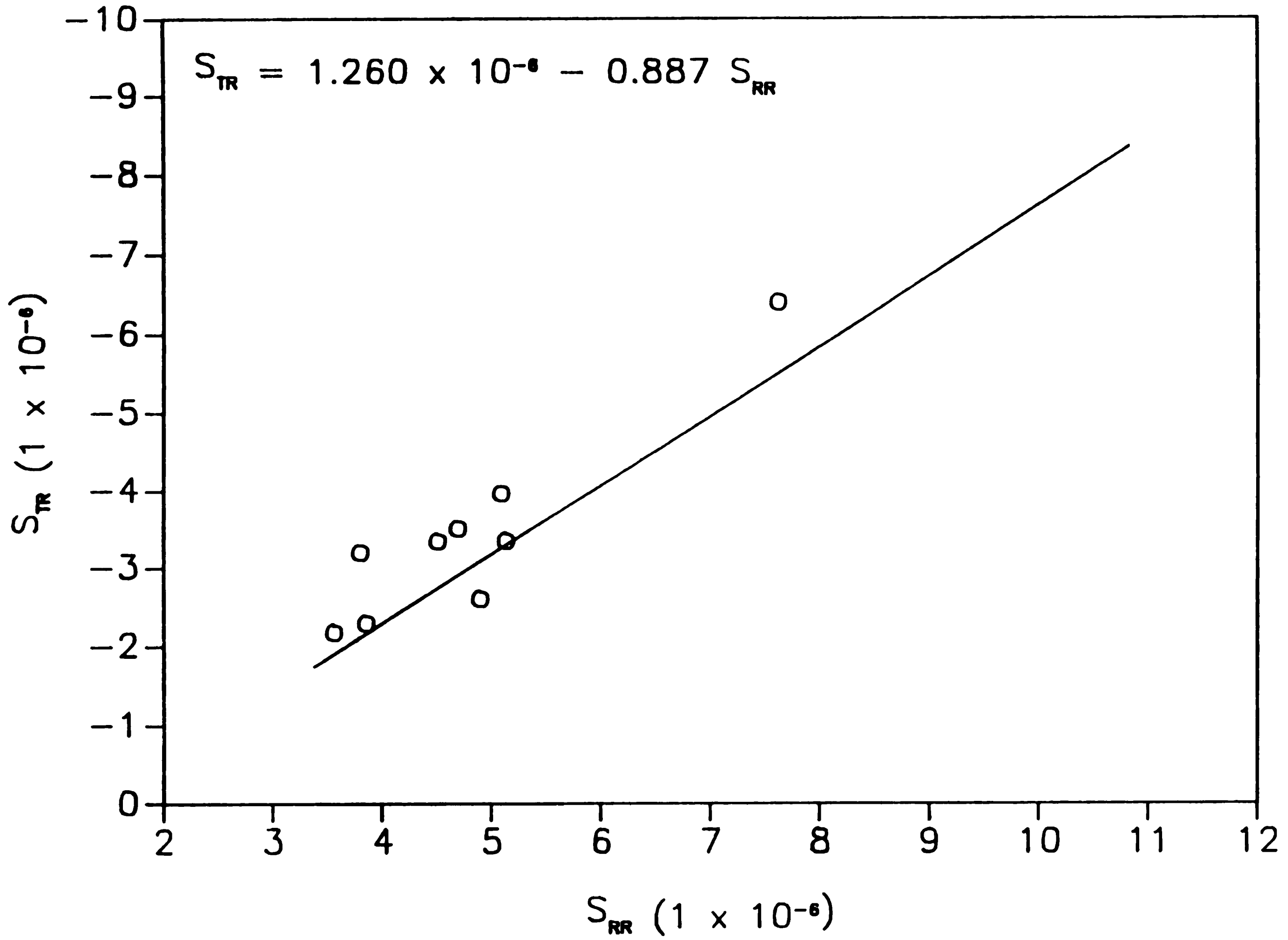

Figure 18. Plotted points showing the relationship between S_{TR} and S_{RR} from this study. The equation derived from Sliker (1988) expressing the relationship between the same two quantities is shown as the solid straight line.

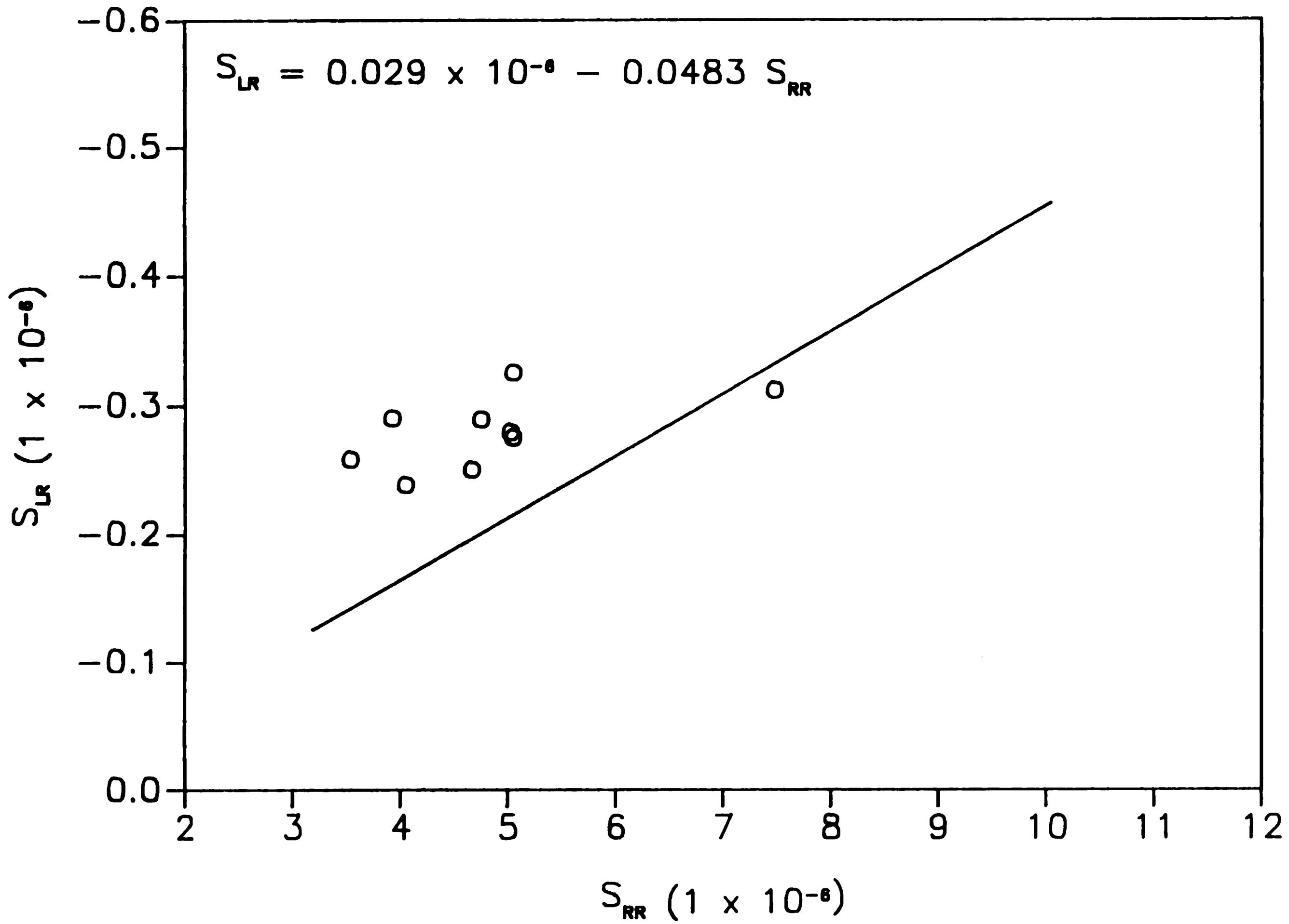

Figure 19. Plotted points showing the relationship between S_{LR} and S_{RR} from this study. The equation derived from Sliker (1989) expressing the relationship between the same two quantities is shown as the solid straight line.

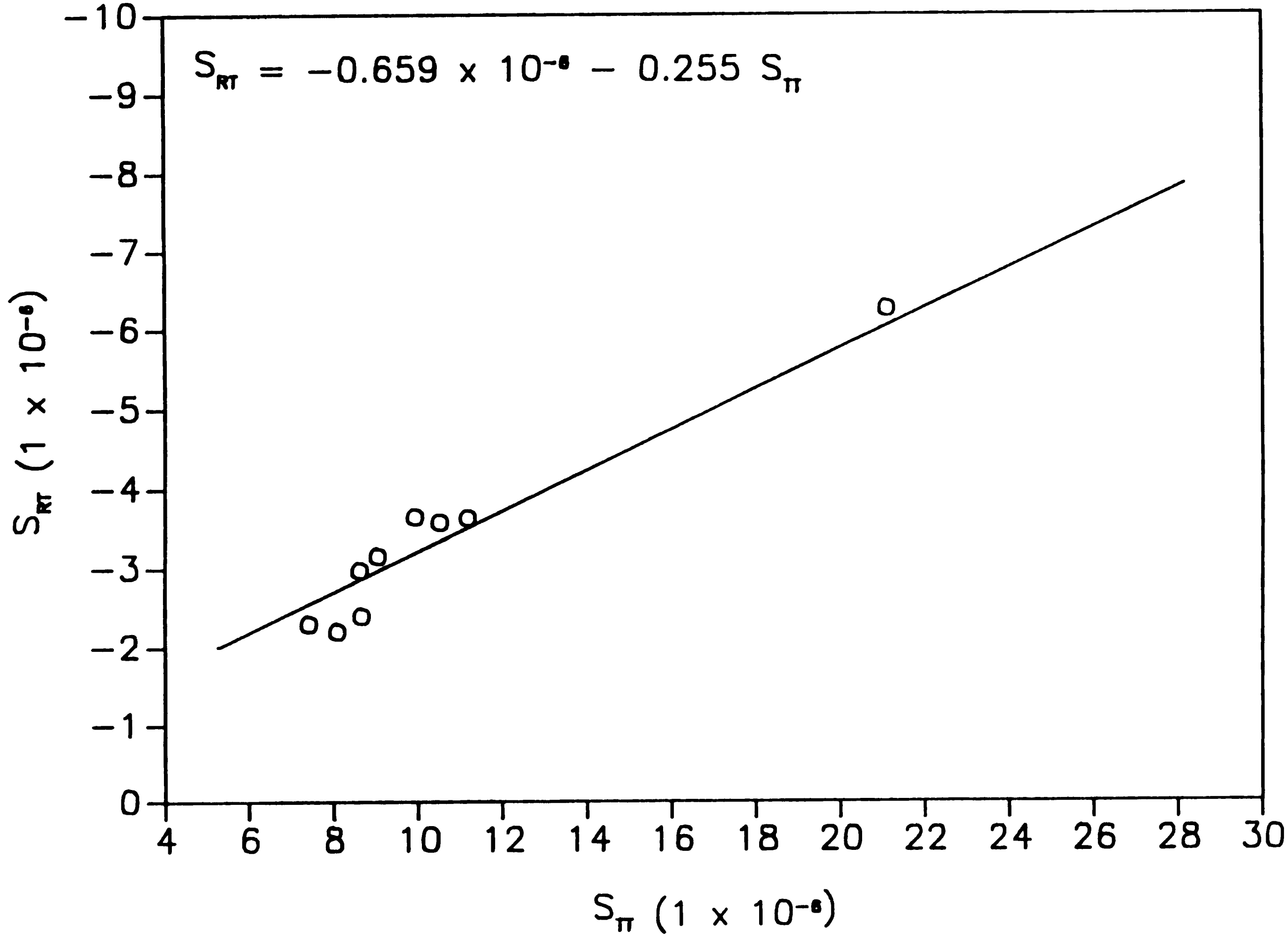

Figure 20. Plotted points showing the relationship between S_{RT} and S_{TT} from this study. The equation derived from Sliker (1988) expressing the relationship between the same two quantities is shown as the solid straight line.

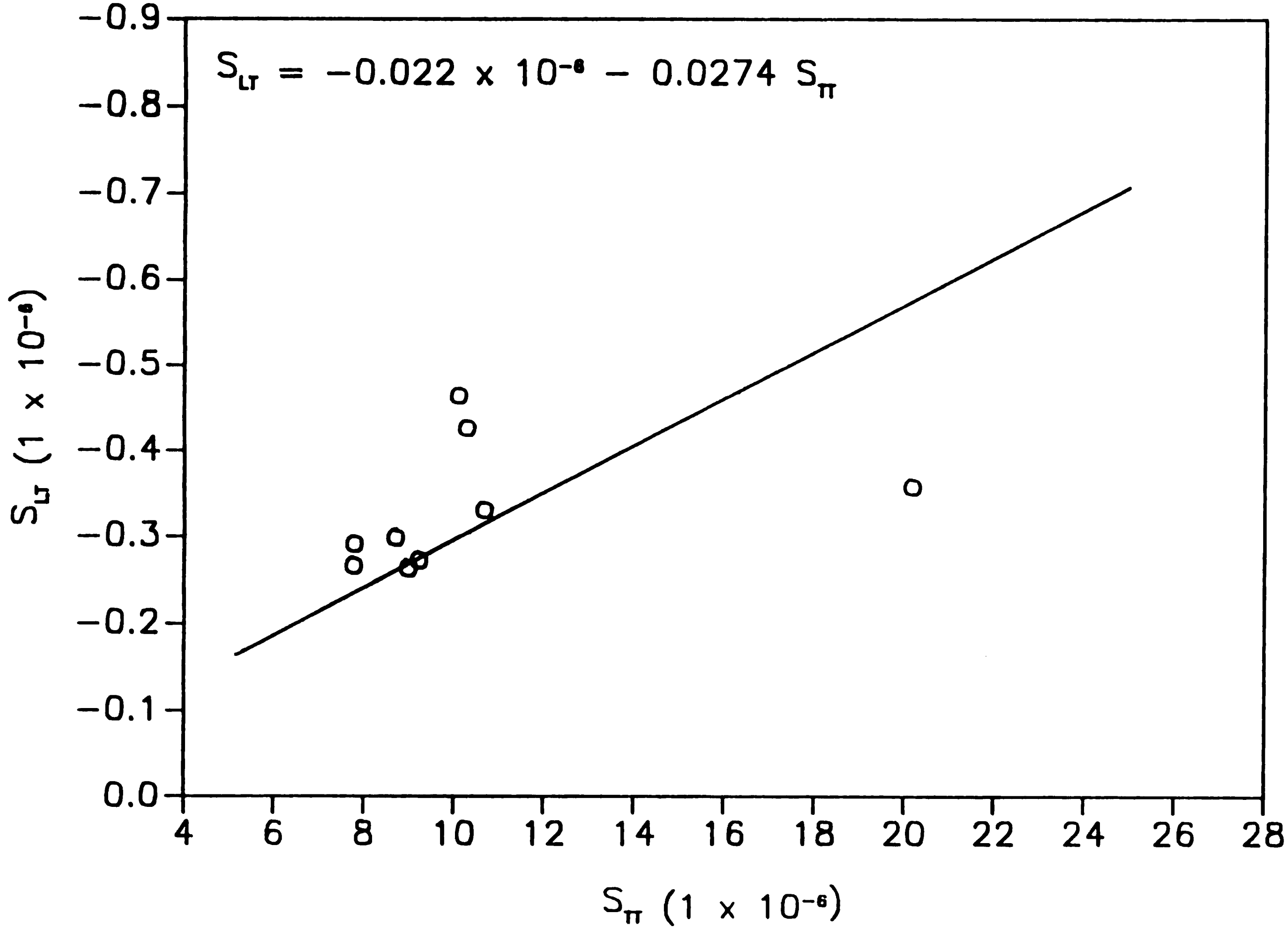

Figure 21. Plotted points showing the relationship between S_{LT} and S_{TT} from this study. The equation derived from Sliker (1989) expressing the relationship between the same two quantities is shown as the solid straight line.

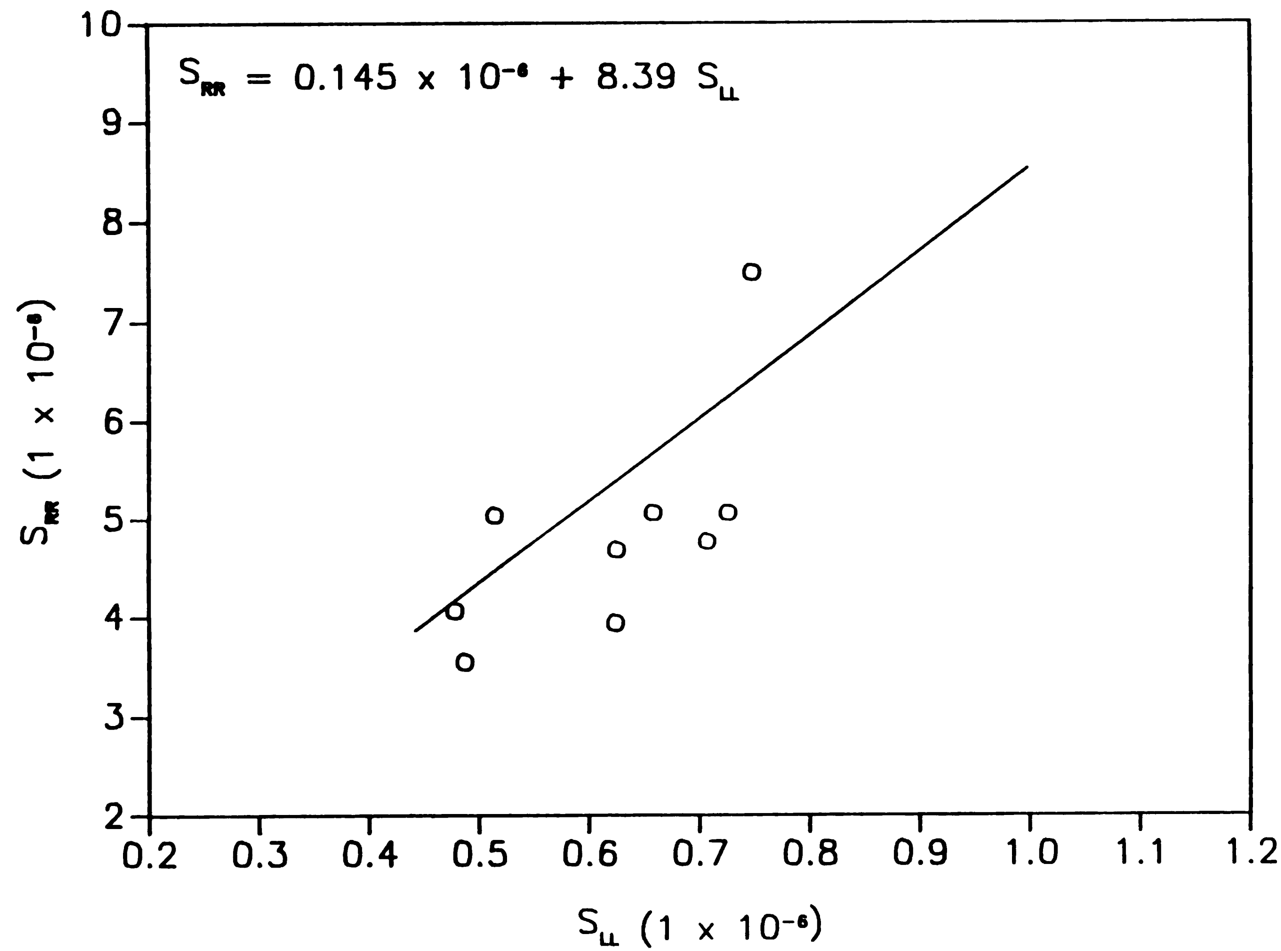

Figure 22. Plotted points showing the relationship between S_{RR} and S_{LL} from this study. The equation derived from Sliker (1985 and 1989) expressing the relationship between the same two quantities is shown as the solid straight line.

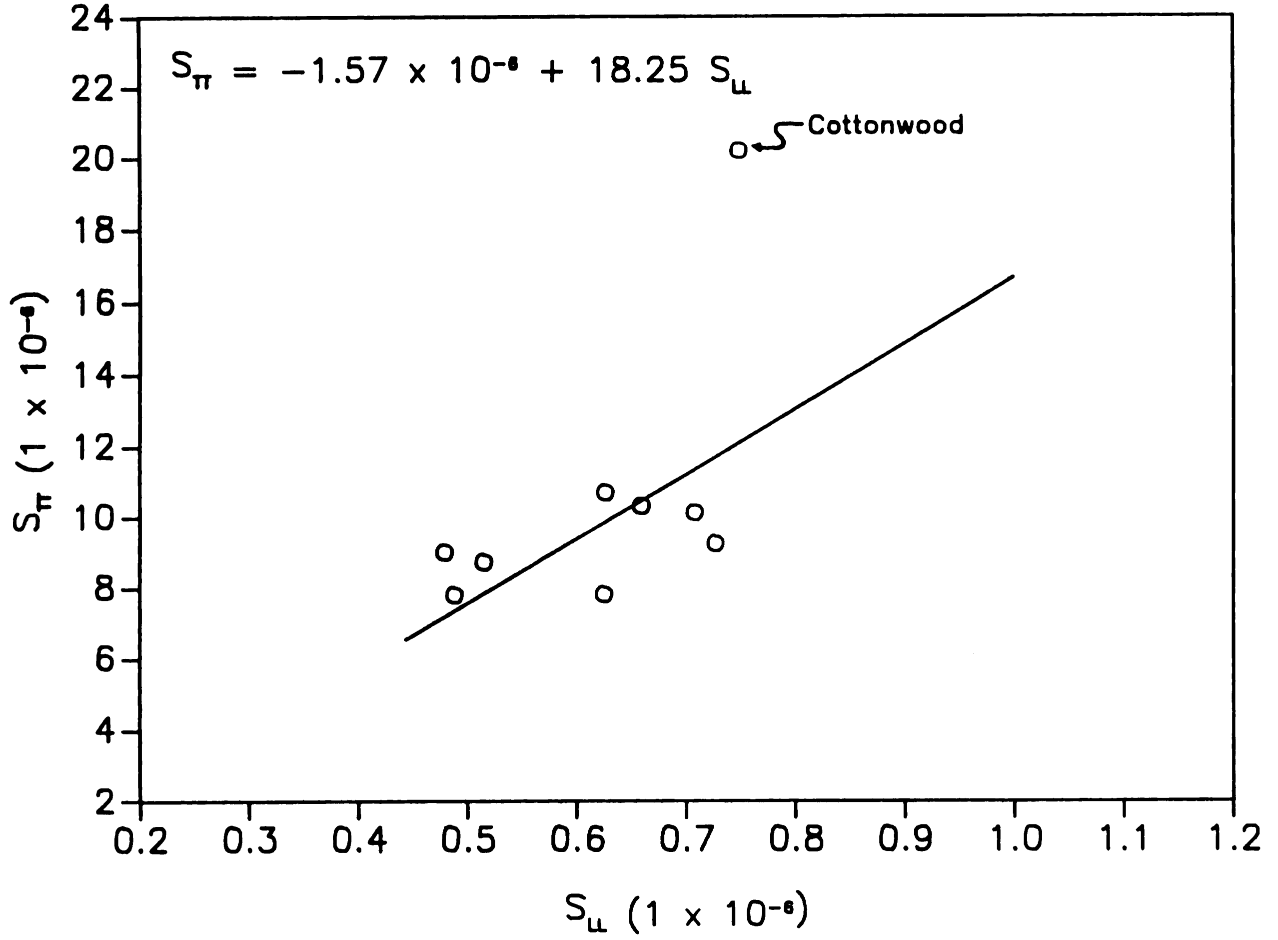

Figure 23. Plotted points showing the relationship between S_{TT} and S_{LL} from this study. The equation derived from Sliker (1985 and 1989) expressing the relationship between the same two quantities is shown as the solid straight line.

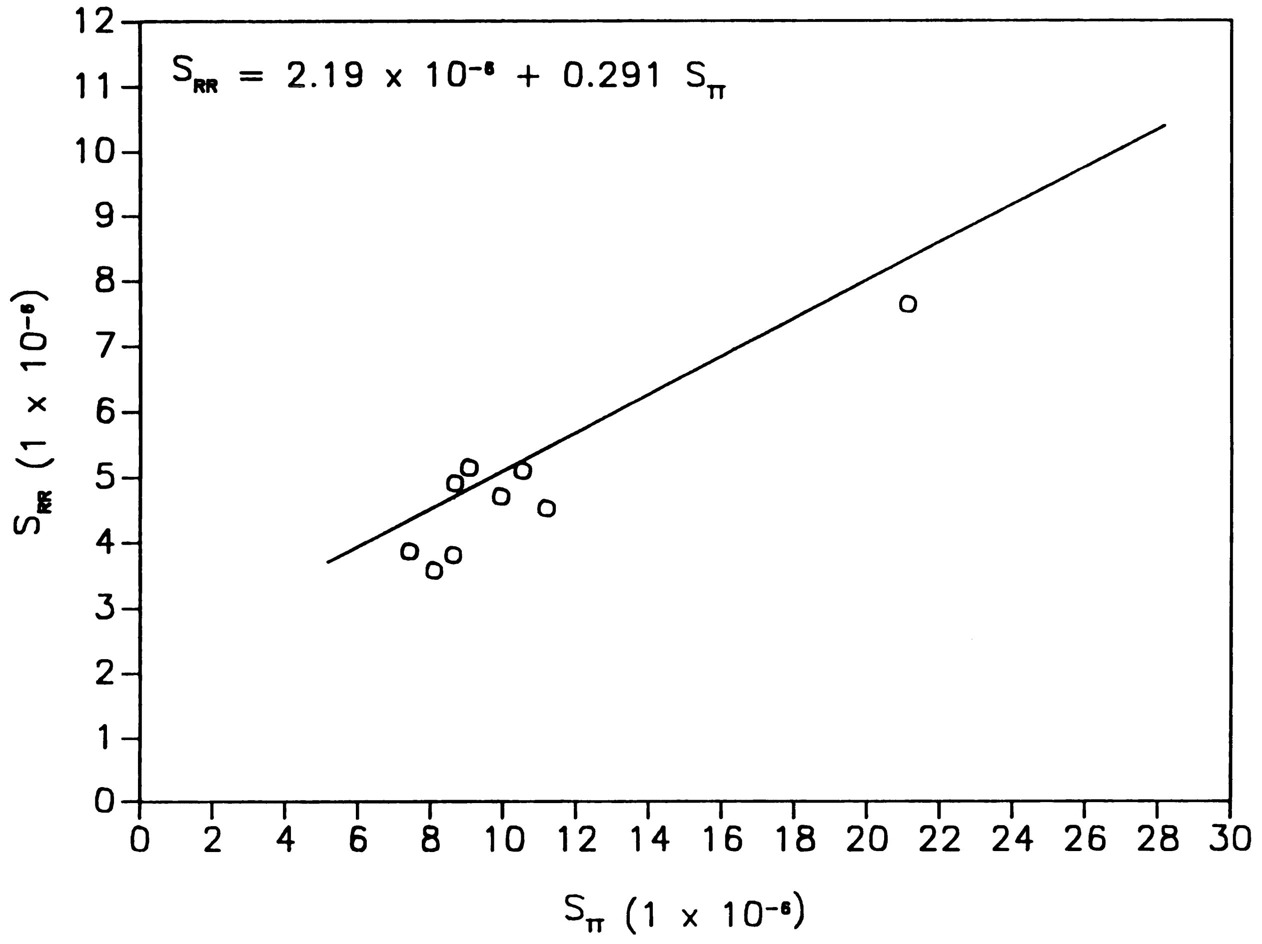

Figure 24. Plotted points showing the relationship between S_{RR} and S_{TT} from this study. The equation derived from Sliker (1988) expressing the relationship between the same two quantities is shown as the solid straight line.

LIST OF REFERENCES

LIST OF REFERENCES

Bodig, J. and J.R. Goodman. 1969. A new apparatus for compression testing of wood. Wood Fiber 1(2): 146-153.

Bodig, J., and J.R. Goodman. 1973. Prediction of elastic parameters for wood. Wood Science, 5(4): 249-264.

Bodig, J., and B.A. Jayne. 1982. Mechanics of Wood and Wood Composites. Van Nostrand Reinhold Company. 712p.

Core, H.A., W.A. Cote, and A.C. Day. 1979. Wood Structure and Identification. Second Edition. Syracuse University Press. 182p.

Guitard, D., and F.EL Amri. 1987. Modeles previsionnels de comportement elastique tridimensionnel pour les bois feuillus et les bois resineux. Ann. Sci. For., 44(3): 335-358.

Panishin, A.J., and C.De Zeeuw. 1970. Textbook of Wood Technology. Third Edition. Volume 1. Structure, Identification, Uses, and Properties of the Commercial Woods of the United States and Canada. McGraw-Hill Book Company. 705p.

Perry, C.C. 1985. Strain-gage reinforcement effects on low-modulus materials. Experimental Techniques, May: 25-27.

Sliker, A. 1959. Electrical resistance strain gages-their zero shift when bonded to wood. Forest Products Journal, 9(1): 33-38.

Sliker, A. 1971. Resistance strain gages and adhesives for wood. Forest Products Journal, 21(12): 40-43.

Sliker, A. 1985. Orthotropic strains in compression parallel to grain test. Forest Prod. J. 35(11/12): 19-26.

Sliker, A. 1988. A method for predicting non-shear compliances in the RT plane of wood. Wood and Fiber Science, 20(1): 44-55.

Sliker, A. 1989. Measurement of the smaller Poisson's ratios and related compliances for wood. Wood and Fiber Science, 21(3): 252-262.

Sliker, A., J. Vincent, W.J. Zhang, and Y. Yu. In press. Compliance equations for wood at three moisture content conditions.

Steel, G.D. Robert and James H. Torrie. 1980. Principles and procedures of statistics. Second edition. McGraw-hill Book Company. 633p.